MONITORING OF GEOTHERMAL BOREHOLE TESTING IN FRAMINGHAM, MA

Sumeet Kumar Sinha

Jiahui Yang

Yaobin Yang

Kenichi Soga

Berkeley
CENTER FOR
Smart Infrastructure

Center for Smart Infrastructure (CSI)
Department of Civil and Environmental Engineering
University of California, Berkeley

ABSTRACT

Shallow geothermal is a renewable green energy that can provide heating and cooling for buildings in a safe, non-emitting, and affordable way, thus reducing the dependence on natural gas. The ground source heat pump (GSHP), also known as a geothermal heat pump, is the most efficient technology to utilize shallow geothermal by transferring heat between the shallow ground and buildings. The Massachusetts 2050 Decarbonization Roadmap mandates zero greenhouse gas (GHG) emissions by 2050. One of the key strategies is thus to electrify building energy using "Networked Geothermal," thus reducing the dependence on natural gas. This report describes the installation, testing, and analysis of temperature measurements using distributed fiber optic sensing (DFOS) on three geothermal boreholes. The tests were part of the pilot project investigating "Networked Geothermal" design and development in Framingham, MA.

Each geothermal borehole was about 600 feet deep and consisted of one U-loop having one supply and a return pipe. The three testing locations were (1) Framingham Fire Station, (2) Farley Parking Lot, and (3) Rose Kennedy, all in Framingham, MA. Fiber optic cables were installed inside and outside the U-loop to monitor changes in the temperature of the circulating fluid (inside the U-Pipe) and the grout (outside the U-pipe). Different installation methods using DFOS were investigated, and their effect on the quality of data obtained was evaluated. The data obtained using DFOS technology had a spatial resolution of 1 m and a temporal resolution of about 4 minutes. An industry-standard thermal response test (TRT) was conducted, where a constant input heat was applied for about 48 hours (referred to as a 'heating phase') with continuous water circulation. After its completion, the input heat and water circulation were stopped. The DFOS continuously took measurements while the water temperature decayed to the surrounding (referred to as the 'decay phase'). The data from the DFOS instrumentation recorded during the TRT test was processed and analyzed to increase the understanding of the boreholes' thermal response and their properties. Finally, the results were used to evaluate the effectiveness of the DFOS technology in monitoring temperature in geothermal boreholes. Important conclusions and recommendations for improvements in future installation, testing, and analysis are also discussed.

Keywords: Distributed fiber optic sensing, geothermal, thermal response test, thermal conductivity

Please use the following citation for this report:

Sinha, S.K., Yang, J., Yang, Y., and Soga, K. (2023). *Monitoring of Geothermal Borehole Testing in Framingham, MA*. Center for Smart Infrastructure, University of California Berkeley. https://doi.org/10.25350/B5J01W

ACKNOWLEDGEMENTS

This work was supported in part by a grant from the Massachusetts Clean Energy Center (MassCEC) to HEET entitled: Learning from the Ground Up. The completion of the work would not have been possible without the support of HEET (Home Energy Efficiency Team). We were grateful to have Asha Nigh supporting the UC Berkeley team throughout the test. We also acknowledge the assistance from Zeyneb Magavi, Angie, Rachel, Carrie, Eric, and Peter. We thank Jared Mullen (Director of Geothermal Operations at Skillings & Sons) and Chris (Geotechnical Engineer at CDM Smith) for their cooperation in the installation and testing of the geothermal boreholes.

DISCLAIMER

Any opinions, findings, conclusions, or recommendations expressed in this material are those of the author(s) and do not necessarily reflect those of the University of California, Berkeley.

TABLE OF CONTENTS

LIST OF FIGURES

LIST OF TABLES

1 INTRODUCTION

1.1 Project Overview

The Massachusetts Decarbonization Roadmap mandates net zero greenhouse gas (GHG) emissions by 2050 (Ismay et al. 2020). Since over a third of the state's emissions come from buildings, electrifying building energy use using renewables is key to this strategy. One such approach is networked geothermal, an innovative solution to heat and cool buildings using interconnected ground source heat pumps. Networked geothermal is safe, non-emitting, and affordable and is the most efficient method currently known for electrifying building space conditioning. In 2016 HEET, a Massachusetts nonprofit climate incubator proposed a utility-scale transition from natural gas to networked geothermal (a gas-to-geo transition pathway) (HEET 2017). They commissioned a study that showed that replacing gas pipes with neighborhood-scale geothermal networks could meet the needs for building heating and cooling throughout most of the state. Figure 1–1 shows an example of a community-based heat pump system where underground pipes filled with water transfer thermal energy between buildings. These geothermal networks can be interconnected to form increasingly large and efficient systems that a thermal distribution utility could manage. HEET's proposal was positively received by utilities and Massachusetts state legislators, and in 2022 Eversource and National Grid received approval from state regulators to install five GeoNet demonstration projects in Massachusetts. The first of these projects, described as the Eversource Project or the Framingham loop, is being installed by Eversource Energy in the city of Framingham, MA. To aid in the design of the Eversource Project, three test boreholes were installed and instrumented at the following locations: (1) Framingham Fire Station, (2) Farley Parking Lot, and (3) Rose Kennedy and the community covered under the Eversource project are shown in Figure 1–2.

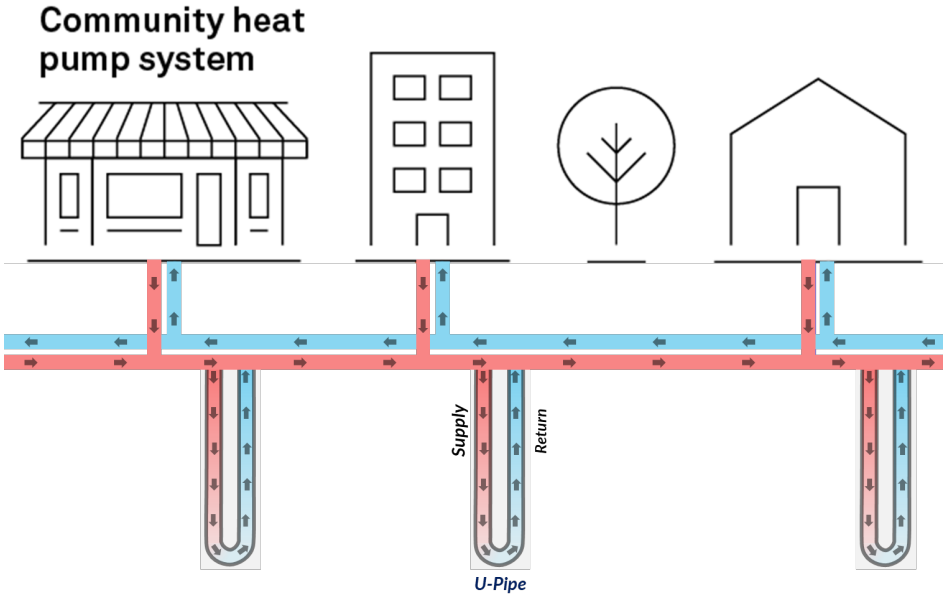

Figure 1–1. Illustration of a community-based heat pump system where the gas pipelines transfer thermal energy between GeoNets and buildings (credit: Cat Weeks, source: Eversource).

Figure 1–2. Overview of the Eversource project showing the three GeoNet locations and the approximate area representing the communities covered.

1.2 Report Summary

This report describes the installation, testing, and analysis of the shallow geothermal boreholes at the three GeoNet locations in Framingham, MA (Figure 1–2). It also evaluates different installation methods and their effectiveness in the quality of data collection. Each geothermal borehole was about 600 feet deep and consisted of one U-loop having one supply and a return pipe, as shown in figure 2. Fiber optic cables were installed inside and outside the U-loop to monitor changes in the temperature of the circulating fluid inside and outside the pipe using the distributed fiber optic sensing (DFOS) technology with a spatial resolution of 1 m. An industry standard thermal response test (TRT) was performed to evaluate the thermal efficiency of the borehole. A primary analysis of the data collected from DFOS technology was performed to evaluate the borehole's geothermal properties, which matched with the conventional TRT test data analysis result. Results show that DFOS effectively monitors temperature changes in boreholes and can be used to estimate the thermal performance of the boreholes at different depths. Finally, recommendations for future installation for long-term monitoring are provided, and directions for advanced numerical analysis are discussed, which can help better understand the geothermal heat exchange leading to more efficient designs.

1.3 Geothermal Boreholes

A GeoNet consists of many geothermal units. Each geothermal unit consists of a circulating fluid flowing through a closed loop that couples the borehole with a heat pump connected to an external infrastructure such as a building. One such closed-loop system uses a U-pipe (see Figure 1–3) where one part of the U-pipe is used to pump heat to the ground (referred to as the supply pipe), and the other pipe is used for extraction (referred to as the return). Figure 1–3 illustrates a geothermal borehole with a U-pipe closed loop system. In this project, the geothermal boreholes were about 600 ft in length and consisted of a standard HDPE U-pipe with an outer diameter of 1.25 inches. Usually, water is used as a medium for thermal energy transportation. Since the heat exchange happens across the water-pipe-grout interface, the grout containing graphite is usually used to increase heat conductivity. Figure 1–3 also illustrates the installation of temperature sensors (for example, fiber optic cables) inside and outside the pipe. The sensor inside the pipe measures the temperature of the circulating water, whereas the one outside measures the grout (or the soil) temperature.

Figure 1–3 shows the fluid's typical thermal response profile (initially with a very high temperature, for example, in summer) as it passes through the U-pipe. When the hot water passes through the supply side of the U-Pipe, it initially has a very high thermal gradient. It thus rapidly dissipates energy to the ground, resulting in a rapid decrease in temperature with depth. While returning, the water (which has already cooled down) can undergo a further decrease in temperature but at a much slower rate due to the decrease in the thermal gradient. As a result, a "V-shaped" temperature profile is obtained where the supply side has a higher temperature gradient than the return side (see Figure 1–3). The overall temperature difference of the water between the supply and the return pipe provides information on the geothermal heat exchange capacity of the borehole, which can then later be used for designing the GeoNets.

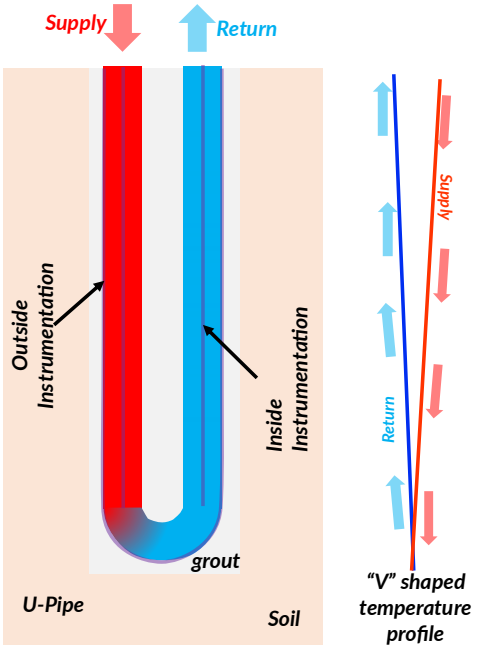

Figure 1–3. An illustration of a geothermal borehole and typical "V" shaped temperature profile of circulating water.

1.4 Thermal Response Test

A thermal response test (TRT) is an in-situ test performed to evaluate the thermal properties (thermal conductivity and thermal resistance) of the geothermal borehole (Gehlin 2002). An illustration of a TRT test is shown in Figure 1–4. In the TRT test, an electric heater applies a constant input heat (Q) to the circulating water, which is continuously pumped through the U-loop. The test is usually carried out for at least 48 hours. The water temperature at the supply end and the return are continuously measured using thermocouple sensors installed inside the TRT Rig. Figure 1–4 shows the plot of time series data of the supply (T_S) and return (T_R) temperatures at the ground surface. Assuming a line source theory, the measured temperature data (T_S and T_R) are processed to determine the thermal properties of the geothermal borehole, which includes borehole thermal resistance (R_b), ground thermal conductivity (λ_g), and ground thermal diffusivity (α_g) (Gehlin 2002). The temperature function (T(t)) can be written as

$$T(t) = \frac{Q}{4\pi\lambda_g}\left[\int_{\frac{r_b^2}{4\alpha_g t}}^{\infty} \frac{e^{-u}}{u}\,du\right] + QR_bT + T_g \qquad \textbf{(1-1)}$$

where,

T(t) is the average of supply and return temperatures (T_S and T_R) at time t (^oF)

H is the active U-Pipe Depth (participating in the heat exchange)

Q is the average heat injected (Btu/hr)

T_g is the undisturbed ground temperature (^oF)

r_b is the average borehole radius (inches)

To measure the undisturbed ground temperature (T_g), the water is circulated in the U-loop for at least 45 minutes (with no heat input) until the temperature of the water reservoir becomes constant. At this state, the supply and return temperatures are equal, i.e., T_S=T_R. In the above Equation, the exponential integral for large values of $\alpha_g t/r_b^2$ can be approximated with the following Equation.

$$\int_{\frac{r_b^2}{4\alpha_g t}}^{\infty} \frac{e^{-u}}{u}\,du = ln\left(\frac{4\alpha_g t}{r_b^2}\right) - \gamma \qquad ,\frac{\alpha_g t}{r_b^2} \geq 5 \qquad \textbf{(1-2)}$$

where,

$\gamma = 0.5772$ is Euler's constant

Combining Equations (1-1) and (1-2), the temperature function can be re-written as,

$$T(t) = \frac{Q}{4\pi\lambda_g}\left[ln\left(\frac{4\alpha_g t}{r_b^2}\right) - \gamma\right] + QR_bT + T_g \qquad , \frac{\alpha_g t}{r_b^2} \geq 5 \qquad \textbf{(1-3)}$$

The ground thermal conductivity (λ_g) can be easily determined from Equation (1-3) by calculating the slope of temperature field T(t) against the natural logarithm of time (i.e., ln(t)). The slope is equal to $Q/4\pi\lambda_g$ for $\frac{\alpha_g t}{r_b^2} \geq 5$.

The ground thermal diffusivity (α_g) cannot be directly determined and is thus estimated by Equation (1-4), assuming a specific heat capacity of ground (c_p)

$$\lambda_g = \alpha_g c_p \qquad \textbf{(1-4)}$$

Once λ_g, α_g, and T_g, are determined, Equation (1-3) can be solved to obtain the borehole thermal resistivity (R_b).

Integrating DFOS with the TRT test can provide information on the variation of temperature along the depth, which can be processed to obtain thermal properties along the depth, eventually leading to the better-informed and efficient design of geothermal boreholes.

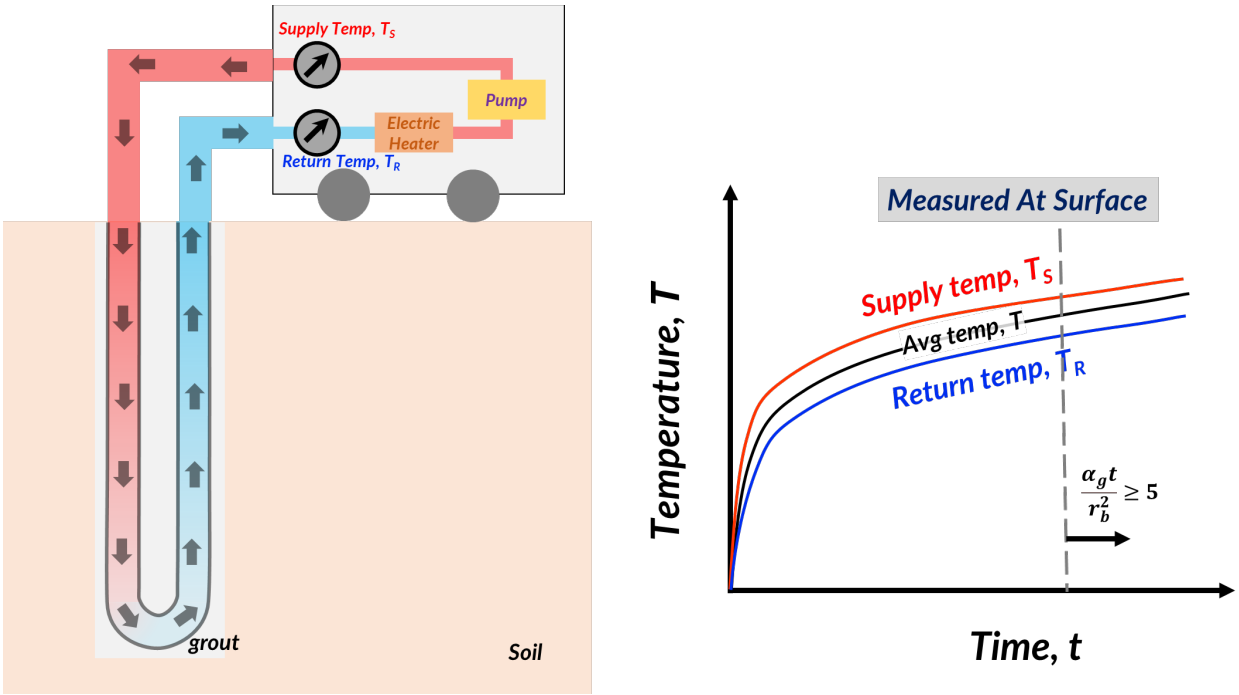

Figure 1–4. An illustration of thermal response test and obtained time series data of return and supply temperature measurement at the surface.

2 GEOTHERMAL BOREHOLES INSTALLATION AND TESTING

2.1 Geothermal Boreholes Installation

Shallow geothermal boreholes about 600 feet deep were installed, one at each GeoNet location, as shown in Figure 1–2. For simplicity and convenience, the boreholes in this report referred to the site locations as "Fire Station," "Farley Parking lot," and "Rose Kennedy" geothermal boreholes. The borehole diameter was about 6 inches. Skillings and Sons (https://www.skillingsandsons.com/) were hired for drilling and installation. Figure 2–1 shows a view of the Fire Station site with a drill rig in operation. The borehole depths, soil layers formation, and ground elevation from the drilling logs in summarized in Table 2–1. A description of the geological materials is given in Appendix A:.

A closed-loop 1-1/4" Aqua-jet HDPE (PE-4710) U-Pipe (from Oil Creek Plastics, https://oilcreekplastics.com/products/) of ASTM D3035 with an outer diameter of 1.660 inches and minimum wall thickness of 0.161 inches was installed inside the boreholes (Figure 2–1). The weight of the U-Pipe was about 27.9 lbs/100" and was rated for 200 psi.

After insertion of the U-pipe, the borehole was grouted with a slurry mixture of GeoPro's thermal grout TGSelect with GeoPro's thermal enhancement PowerTEC (https://geoproinc.com/). The grout mixture design used 150 lb of TGSelect and 64 lb of PowerTEC with 48 gallons of water, resulting in a design thermal conductivity of 1.4 Btu/hr-ft-°F. The properties of the grout used are summarized in Table 2–2. The grout was left to cure for at least three days before the TRT test was performed.

Table 2–1. Summary of borehole depth and layer formation.

Layers Thickness (feet)	Formation Description	Total depth (feet)	Elevation (feet)
Fire Station Borehole			
84	Overburden (brown cobbles, fine sand)	610	173
526	Grey Diorite, Gabbro		
Note: Bore produced 8 gpm water at 233-236 ft			
Rose Kennedy Borehole			
136	Overburden (brown cobbles, boulders, and clay)	610	202.3
474	Grey Diorite		
Note: Bore produced 2 gpm water at 460-480 ft.			
Farley Parking Lot Borehole			
60	Overburden (brown and gray boulders and silty clay)	615	172.5
555	Light gray, gray, and pink Diorite		
Note: Boulders from 53-60 ft made casing installation difficult. Bore also produced 2 gpm water from 460-480ft.			

Table 2–2. Grout mix design and properties (reference: https://geoproinc.com/products/thermalGroutSelect.html).

Grout Mix Design	Design Thermal Conductivity	Density (lb/gal)	Permeability (cm/s)
150 lb TGSelect, 64 lb PowerTEC, and 48-gal water	1.4 (Btu/hr-ft-^{o}F)	10.7	$<1x10^{-7}$

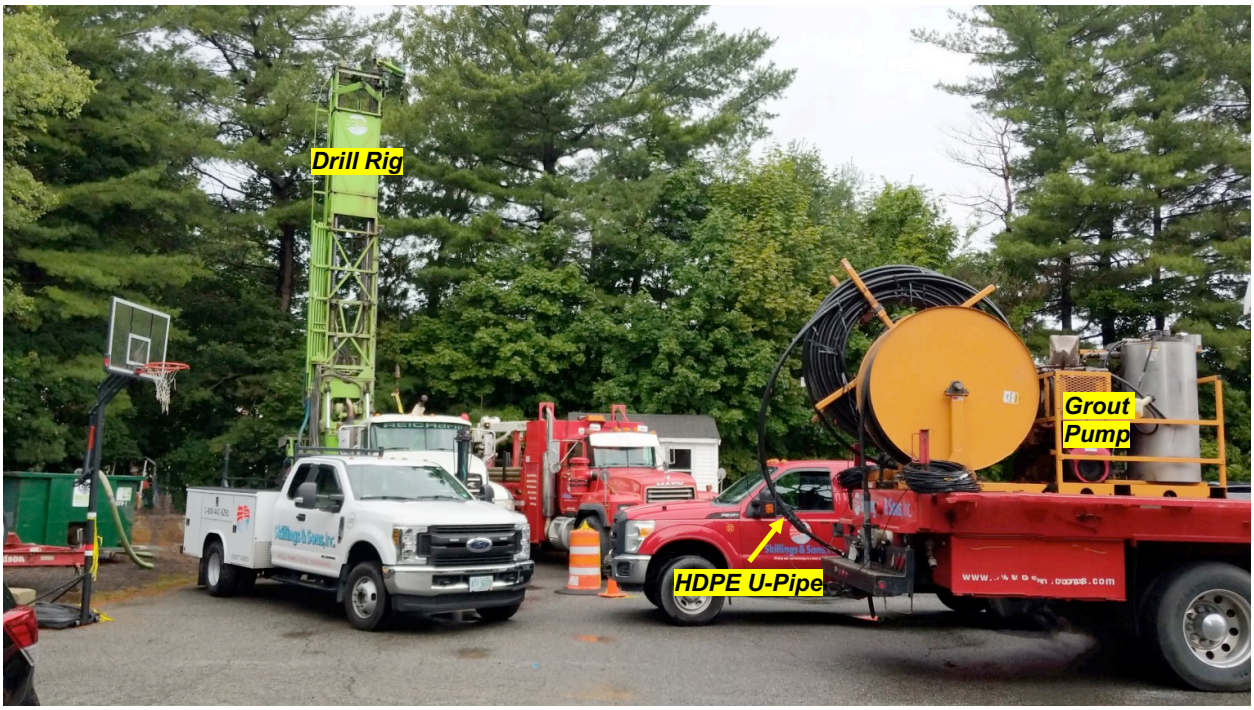

Figure 2–1. A view of the Fire Station site.

2.2 Instrumentation

The U-pipes were instrumented with fiber optic cables to measure temperature along the depth. Two types of instrumentation were performed: one outside the U-pipe and one inside the U-pipe, as shown in Figure 1–3. The outside instrumentation was performed in all the boreholes, whereas the inside instrumentation was only performed at the Fire Station site.

The instrumentation was attached outside and inside the U-Pipe. Table 2–3 summarizes the instrumentation in the boreholes and the attachment quality. The outside instrumentation was applied on all the boreholes. However, their quality differed across different boreholes as specified in Table 2–3. The inside instrumentation was only applied for the Fire station borehole. The description of the instrumentation procedure for inside and outside the U-Pipe are described later in Sections 2.2.2 and 2.2.3, respectively. Section 3 describes the effect of instrumentation quality on the data obtained during thermal response tests.

Table 2–3. Summary of instrumentation at the three boreholes and their quality.

Borehole	Instrumentation	Outside Instrumentation Attachment Quality
Fire Station	Inside as well as Outside	Bad: U-pipe twisted thrice, electric tape attachment at very large separation length (> 10 feet). The FO cable length outside the borehole at the supply and return pile was unequal by about a meter.
Rose Kennedy	Outside	Very Good: electric tape attachment at about every 3 feet, no twisting
Farley Parking Lot	Outside	Good: electric tape attachment at about every 3-6 feet, U-pipe twisted once

2.2.1 Fiber Optic Cable

The fiber optic (FO) cable used for instrumentation was Belden temperature cable FSSC002N0 (https://www.belden.com/). The properties of the Belden FO temperature cable are summarized in Table 2–4, and its cross-section is shown in Figure 2–2. Each FO consists of two cores loosely bonded in a gel-filled tube. The two cores can be used independently to measure temperature changes along the cable.

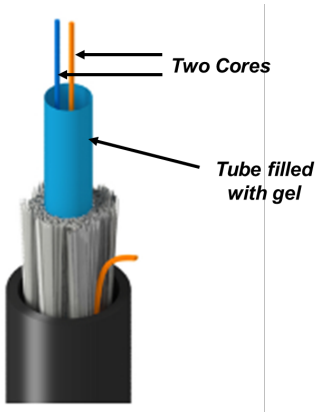

Figure 2–2. View of the inside of the Belden temperature fiber optic cable FSSC002N0 (credits: Belden.com).

Table 2–4. Properties of Belden temperature fiber optic cable.

Properties	Values
Outside Diameter (OD)	0.15 inch
Minimum Bending Radius	15 OD
Maximum Tensile Strength	180 lbf
Bulk Cable Weight	33 lb/kft
Operation Temperature Range	-40 - 70 ºC
Temperature Coefficient	1.1 MHz/ºC

2.2.2 Outside Instrumentation

The FO cables were first attached at the bottom of the U-pipe, as shown in Figure 2–3. The 0.15-inch OD temperature FO cable, having a larger turning radius, was spliced with a 2 mm FO cable to make the U-turn. The FO cables were attached to the U-pipe using electric tape. Results from Optical Time Domain Reflectometer (OTDR) showed that the sharp U-turn at the bottom of the U-pipe (even after using a smaller diameter FO cable) resulted in signal loss. It was also found that applying a very tight attachment further increased signal loss. So, the tape was not applied gently to reduce the signal loss. In addition, double-sided tapes were used to provide cushion at the interface between the cable and the pipe during the U-turn.

The rest of the outside instrumentation (see Figure 1–3) was applied in flight while the U-pipe was inserted in the borehole. The FO cables were attached using electric tape at specific intervals. The installation involved at least two people, one holding the FO cables in position and the other applying the tape. Ideally, attaching the tape at every 3 feet was desirable to make the FO cable in contact with the U-Pipe. However, this involved stopping the insertion operation at regular intervals. With the current equipment for inserting U-pipe and other practical concerns, it was difficult to stop the U-pipe insertion at regular intervals and thus maintain a constant length between positions of tape application. Also, sometimes the U-Pipe twisted inside the borehole, making the cable attachment even more difficult. As a result, the quality of installation for the outside cable varied for different sites, as summarized in Table 2–3. The Fire Station site being the first site, the cable attachment did not go well. The electric tape was applied at a larger separation length (more than 2-3 m), and the U-Pipe was twisted thrice during the installation. For the following two sites, the installation went relatively well. The quality of the outside instrumentation was very good at the Rose Kennedy site because it was possible to attach the cable with tapes at about every 3 feet. The instrumentation quality at the Farley parking lot was also relatively good.

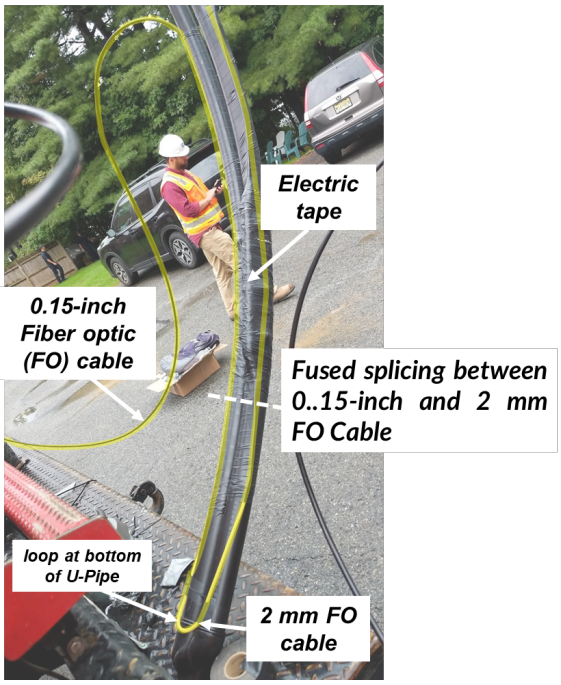

Figure 2–3. A view of the outside instrumentation showing the fiber optic cables attached to the bottom of the U-Pipe.

2.2.3 Inside Instrumentation

The two cores inside the temperature FO cable were fusion-spliced together, as shown in Figure 2–4, and then inserted inside each of the supply and return pipes (of the U-Pipe) using VEVOR fish tape fiberglass (https://www.vevor.com/duct-rodder-fish-tape-c_10773/200m-656ft-fish-tape-6mm-fiberglass-wire-cable-running-rod-duct-rodder-puller-p_010711189415), after the U-pipe was inserted into the borehole. A steel spoon (see Figure 2–4) was designed to glue the bare FO cable, protect the splicing, and hook the fish cable for inserting into the U-Pipe. The drawing of the spoon is shown in Figure 2–5. Since the two cores independently measured the same temperature, their average values were taken during processing to record the inside temperature of the supply and return pipe of the U-Pipes (see Figure 2–4). A FPT Brass T-joint (1-1/4" x 1-1/4" x 1") was used to route the inside instrumentation outside the U-pipe. Silicone grease was attached to prevent water leakage during the thermal response test.

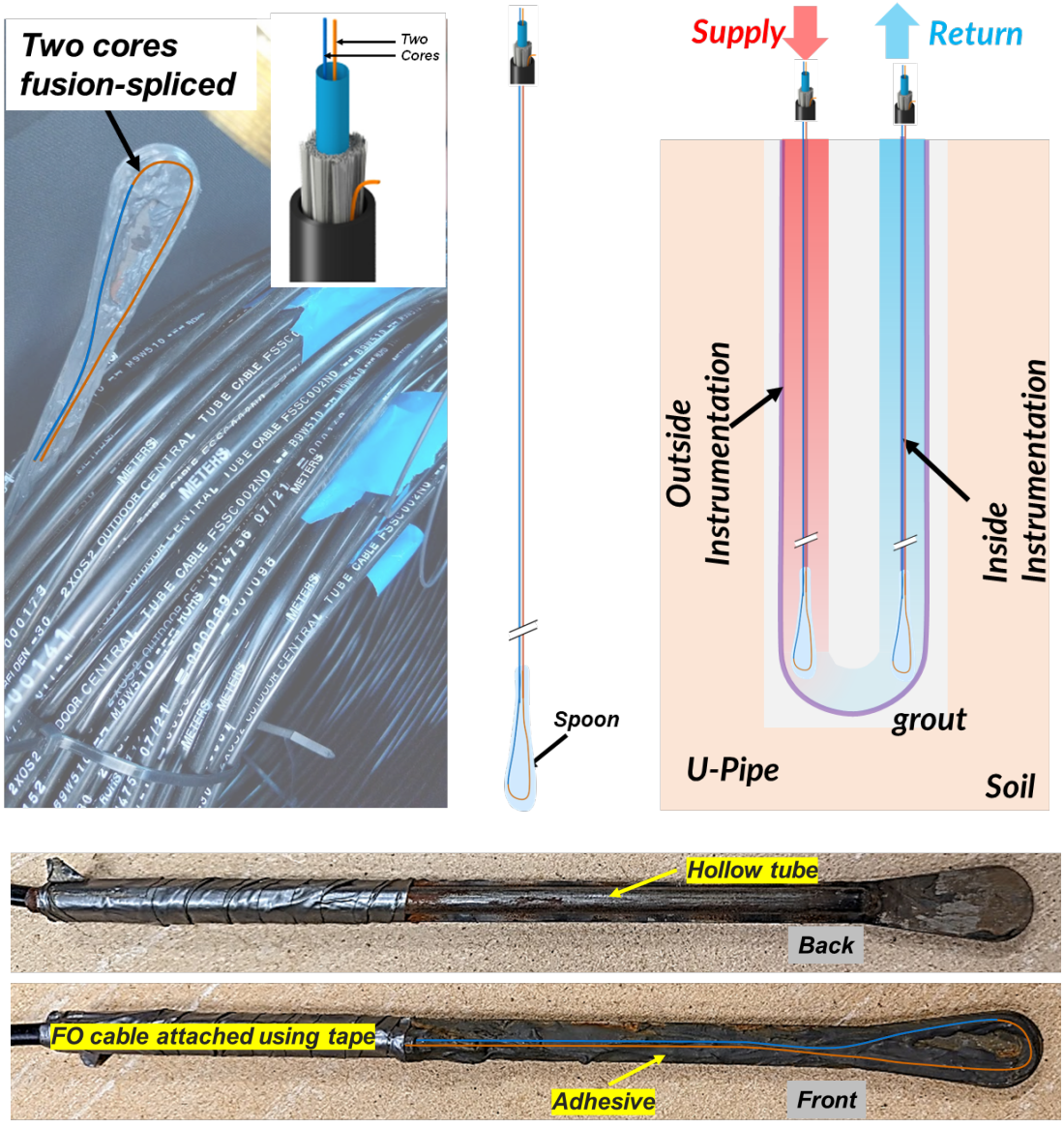

Figure 2–4. A view of the FO cable prepared for inside instrumentation.

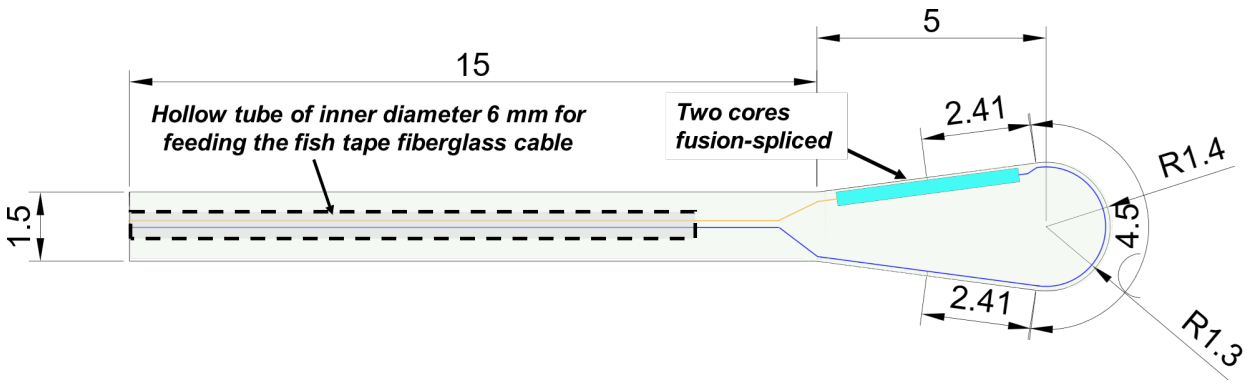

Figure 2–5. Design of the spoon. All dimensions are in cm unless explicitly stated.

2.3 Thermal Response Testing

A thermal response test (TRT) was performed on all the geothermal boreholes. Section 1.4 briefly describes the TRT test. The test procedure is described in Appendix B:. Figure 2–6 shows the view of the set-up during the thermal response test. The timeline for the borehole installation and TRT testing are summarized in Table 2–5. The TRT test was carried out (with constant input heat) for about 47-48 hours. Following that, the heating elements were turned off; however, the temperature using DFOS was continuously monitored for at least 4 hours or more (see Table 2–5). The TRT test phases are thus referred to as the "heating" and "decay" phases, depending on whether the heating elements are turned on or off. An electric pump continuously circulated water in a closed loop during the heating phase. However, during the decay phase, the pump was turned off, and thus water remained stagnant. Figure 3–1 shows the supply and return temperature data near-ground surface during the heating and decay phases.

During the TRT test, the temperature in the FO cables was continuously monitored using a Brillouin Optical Time Domain Analysis (BOTDA) analyzer. The BOTDA analyzer used was Omnisens' DITEST STA-R Series analyzer (see Figure 2–6). Hu et al. (2021) describe the BOTDA technology. BOTDA technology measure change in temperature but not the absolute temperature. BOTDA uses the change in Brillouin frequency from the scattered signal within the FO cable to detect temperature changes. The change in Brillouin frequency to temperature change has a linear relationship, given by the temperature coefficient of the FO cable (see Table 2–4). The spatial resolution and accuracy of the temperature measurement were about 3 feet and 1° C (1.8 °F), respectively. The sampling rate of the measurement was variable. The analyzer took at least one or more measurements within 8 minutes. The spatial sampling rate was 1 reading about every 1.34 feet. Simultaneously thermocouple sensors installed inside the TRT rig measured the temperature of the circulating water at the surface (Figure 1–4).

Table 2–5. Timeline of borehole installation and thermal response test.

Date (EST)	Event Description
Fire Station Borehole	
9/22/2022	Installation of the U-Pipe with outside instrumentation
10/11/2022	Installation of inside instrumentation
10/17/2022 - 10/19/2022	Thermal response test - with constant heat input rate = 47.4 hr - with heating coils turned off = 4.4 hr
Rose Kennedy Borehole	
9/28/2022	Installation of the U-Pipe with outside instrumentation
10/19/2022-10/21/2022	Thermal response test - with constant heat input rate = 47.0 hr - with heating coils turned off = 11.5 hr
Farley Parking Lot Borehole	
9/22/2022-9/23/2022	Installation of the U-Pipe with outside instrumentation
10/13/2022 - 10/15/2022	Thermal response test - with constant heat input rate = 47.9 hr - with heating coils turned off = 24 hr

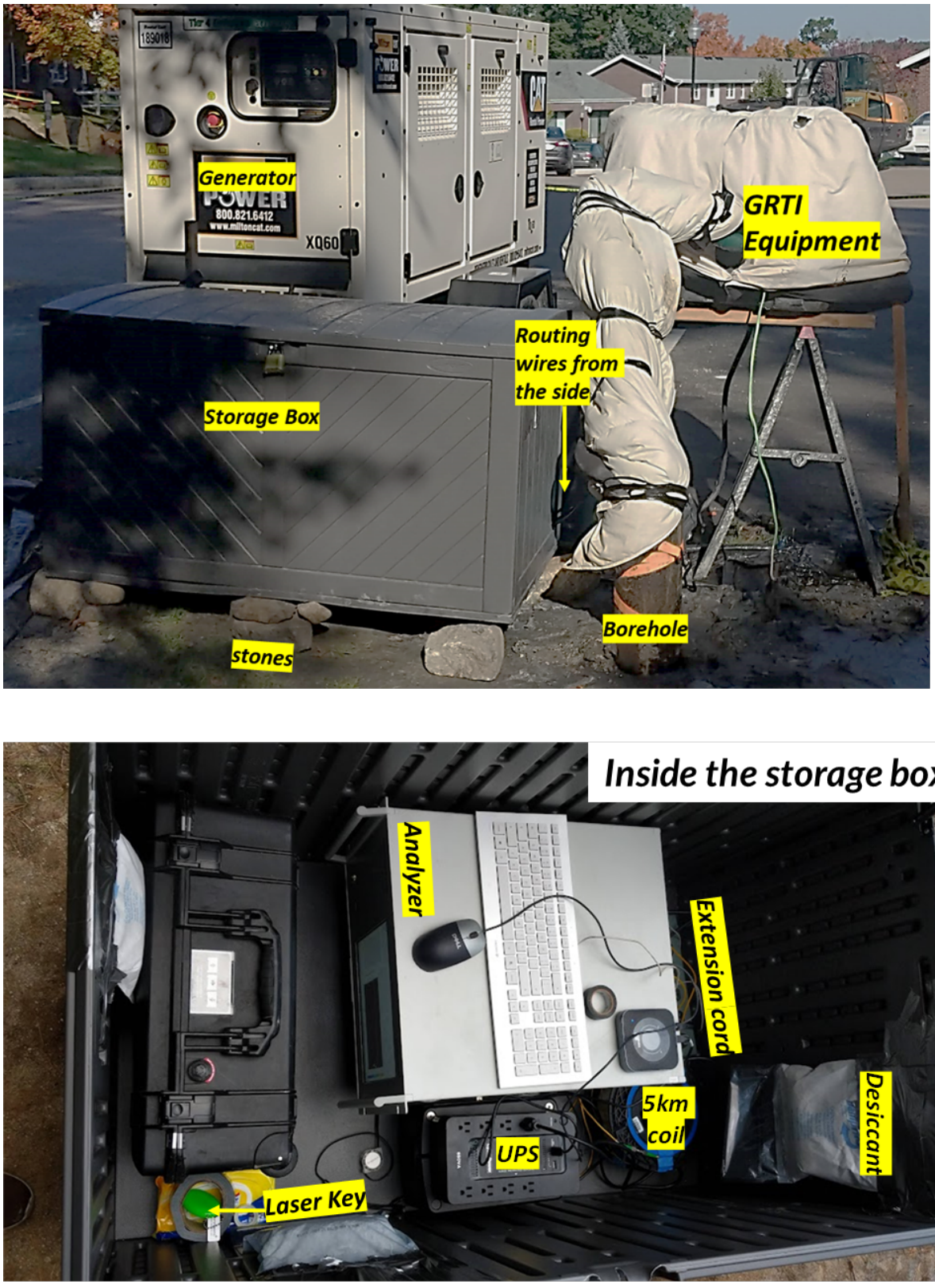

Figure 2–6. View of the set-up during the thermal response testing at the Rose Kennedy borehole.

3 RESULTS FROM THE THERMAL RESPONSE TESTS

Results from the DFOS provided a time history of temperature change at different depths and temperature profiles at various times during the heating and decay phase. Figure 3–1 illustrates the temperature profile measured (from the outside instrumentation) at selected times during the heating and decay phase of the TRT test on the Farley Parking Lot geothermal borehole. It also shows the time history of temperature change at the near surface in the supply and return pipes. It can be seen from the plots that during the heating phase, the temperature profile is in the V-shaped curve, as described in Section 1.4. DFOS measurements were processed to obtain the thermal properties of the geothermal borehole and were compared with the GRTI analysis. The analysis procedure is described in Appendix B: and Section 1.4. The subsections below describe the processing and results of DFOS data for each borehole.

It should be noted that the DFOS outside instrumentation measured the temperature change (ΔT) of the grout surrounding the U-Pipe. In contrast, the inside instrumentation measured ΔT of the circulating fluid inside the U-Pipe. The thermocouple sensors installed inside the TRT Rig measured the surface temperature of the fluid circulating in the U-Pipe. It is expected that at the ground surface, ΔT in water (as measured by the TRT rig thermocouples) would be much higher than the ΔT in the grout (measured by the DFOS outside instrumentation).

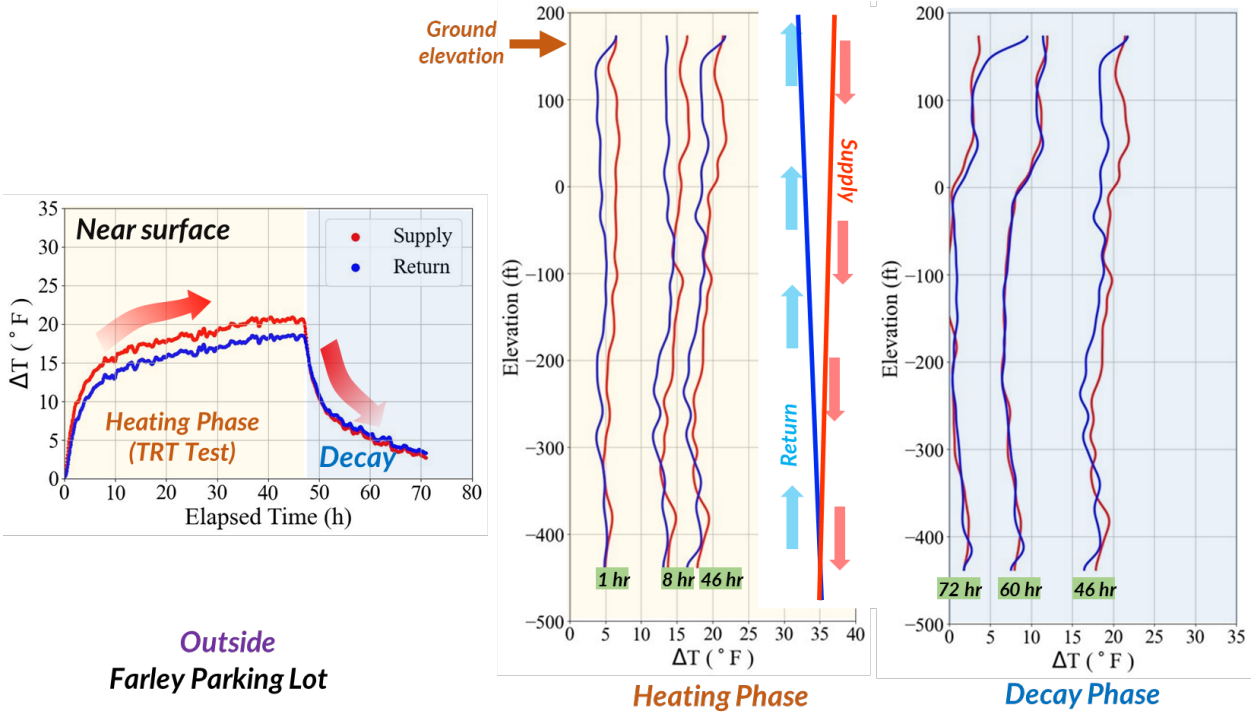

Figure 3–1. Illustration of measurements recorded from DFOS Outside instrumentation during the TRT test (conducted at the Farley Parking Lot): Results on the time history of changes in temperature measurement in the supply and return pipe and temperature profile plots at different times during the heating and decay phase.

3.1 Farley Parking Lot Geothermal Borehole

A TRT test was conducted on the Farley Parking Lot borehole on Oct. 13 – 15, 2022. The full GRTI report describing the test statistics and analysis is provided in Appendix C:. Table 3–1 summarizes the test statistics.

The sampling rate was about 4 mins. The heating and decay phases were ~ 47.9 hours and 24 hours, respectively. Figure 3–2 shows the 2D contours of temperature change (ΔT) versus depth and time. To reduce noise and analyze the spatial-temporal characteristics, the raw ΔT data (Figure 3–2 (a)) were filtered using a 2D anisotropic Gaussian Filter with σ_{time} of 3 and σ_{depth} of 9 (Figure 3–2 (b)). The filtered data was used to analyze the temperature profile and time history at different depths and times, respectively.

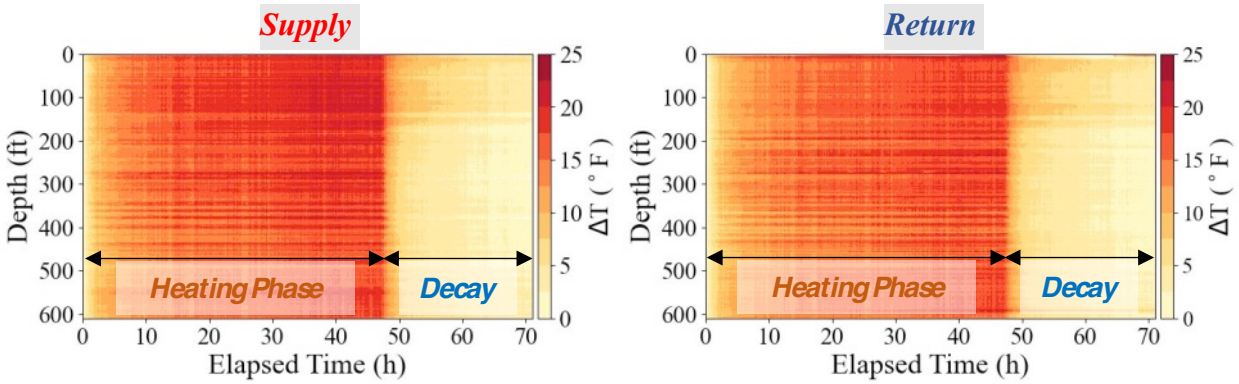

(a) Raw Data

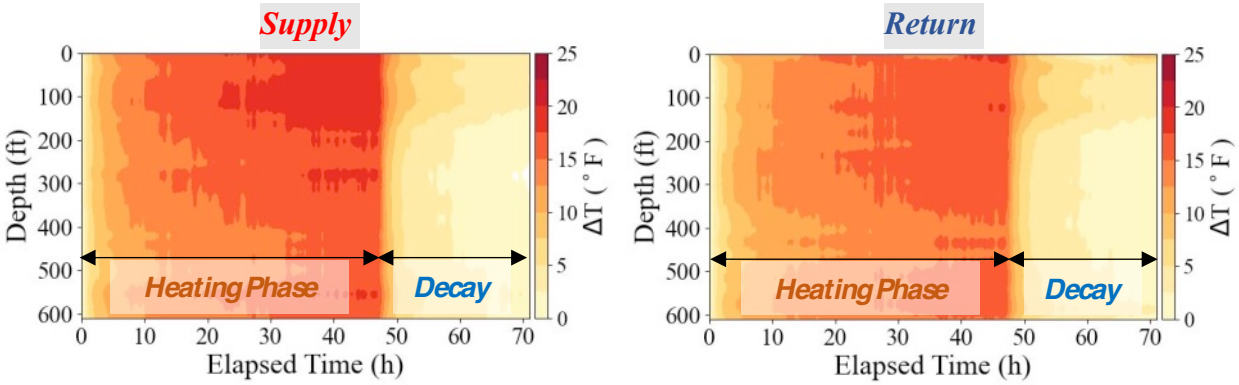

(b) Filtered Data

Figure 3–2 2D Contours of temperature change (ΔT) showing (a) raw and (b) filtered data with depth and time from the DFOS Outside instrumentation during the thermal response test conducted at the Farley Parking Lot geothermal borehole.

Table 3–1. Thermal response test statistics for Farley Parking Lot geothermal borehole.

Parameter	Values
Undistributed Formation Temperature	53.3 – 54.1 °F
Duration	47.9 hours
Average Voltage	238.7 V
Average Heat Input Rate	32138 Btu/hr (9416 W)
Average Heat Input Rate Density	53.3 Btu/hr-ft (15.3 W/ft)
Circulator Flow Rate	12.3 gpm
Standard Deviation of Power	0.05 %
Maximum Variation in Power	0.19 %

3.1.1 Time Histories and Profiles of Temperature Change (ΔT) Measurement

The filtered data was processed to investigate the temperature change (ΔT) time histories at selected depths. The ΔT time histories at selected depths of 50 ft, 200 ft, 300 ft, and 500 ft are shown in Figure 3–3. The total temperature increase near the surface (about 50 ft) was about 15 – 18 °F. As expected, the change in the supply temperature (ΔT_{supply}) is usually higher than ΔT_{return} (Figure 3–3). The total difference between ΔT_{supply} and ΔT_{return} near the surface was roughly 3 °F, which decreased with depth and ultimately converged to zero (at about 500 ft).

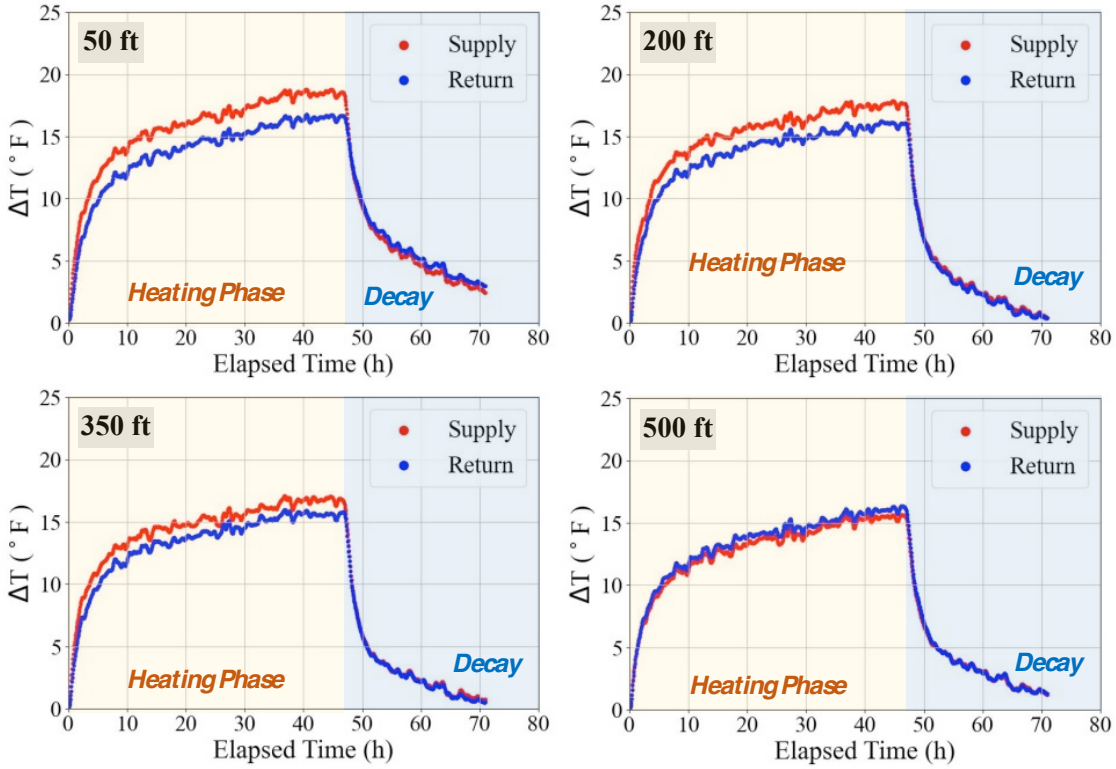

Figure 3–3 Recorded temperature change (ΔT) time-histories at selected depths from the DFOS Outside instrumentation during the thermal response test conducted at Farley Parking Lot geothermal borehole.

The filtered data was also processed to investigate the temperature change (ΔT) time histories at selected times during the heating and the decay phase. The ΔT profiles at selected times during the heating and decay phase are shown in Figure 3–4. The figure shows that ΔT_{supply} is usually higher than ΔT_{return}, but the difference decreased with depth, leading to the formation of the "V" shape, as described in Section 1.4. Towards the end of the heating phase, ΔT at shallow depths increased by 17 – 20 °F, while at the bottom of the borehole, it only increased by 15 °F. It is worth noting that the ΔT_{supply} and ΔT_{return} converge at a depth of 250 ft and below the depth of 500 ft, indicating that the heat transfer efficiency from the borehole to the ground at these locations is low. A possible reason could be the poor quality of grouting or the entanglement of the fiber optic cables resulting in similar ΔT_{supply} and ΔT_{return} measurements. During the decay phase, water circulation stops, and the heat from the water dissipates in the surrounding soils. As a result, the difference between ΔT_{supply} and ΔT_{return} decreased quickly and ultimately converged over itself within a few hours, as shown in Figure 3–3 and Figure 3–4. The temperature of the return and supply cable converged within 1 hour.

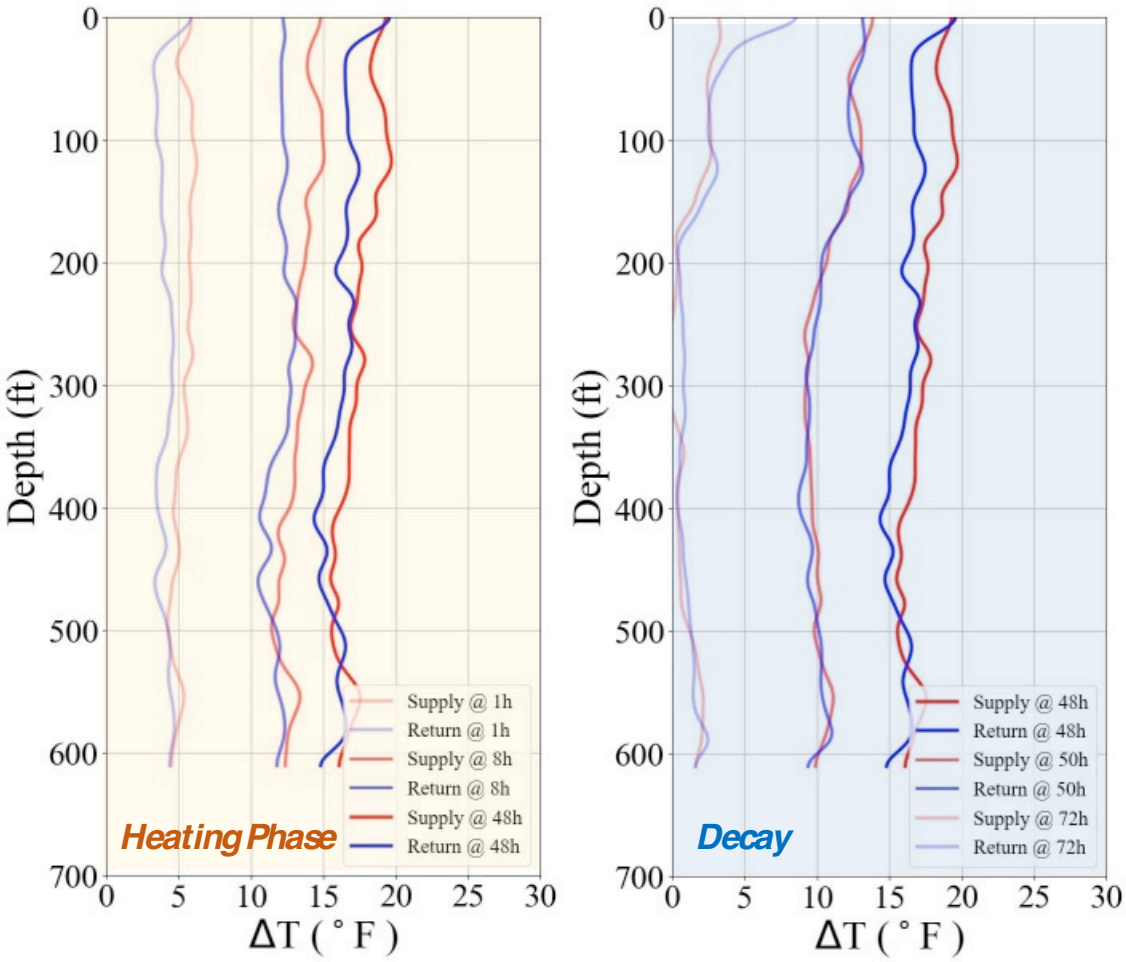

Figure 3–4 Profiles of temperature change (ΔT) at selected times during the heating and decay phase as recorded from the DFOS Outside instrumentation during the thermal response test conducted at the Farley Parking Lot geothermal borehole.

Fluctuation of ΔT can be observed in both supply and return pipes. Several reasons can potentially contribute to this, among which the most important is the variation in grouting quality along the depth. Grouting quality can affect the heat transfer efficiency between the U-Pipe and the surrounding soil, leading to a variable temperature profile. Another major factor could be the variable position of the fiber optic cable surrounding the U-pipe arising from either twisting of the U-Pipe, slack in the fiber optic cable, or from longer and non-uniform tape attachment positions during the installation. The geological condition and water flow direction can also affect the ΔT temperature due to the variation of the thermal conductivity in the soil layer. Since the installation of the borehole was relatively good, the possible reason for any fluctuation in the data could be the poor quality of grout or geological conditions.

The linearity and the slope of the ΔT in natural log time can be used to understand the thermal properties of the borehole (see Equation (1-3)). Figure 3–5 investigates the linearity of ΔT time histories in natural log time at selected depths during the heating and decay phases. Table 3–2 summarizes the temperature data's linearity with the natural time log for the stable regions within the heating and decay phase. The stable regions within the heating phase constitute the data after 10 hr. For the decay phase, the stable data is after the temperature of the supply, and the return pipes converge, i.e., after 1 hr. Results from the table show strong linearity during the heating phase. However, the slopes are slightly different at different depths indicating the variable thermal conductivity with depth. In the decay phase, linearity decreases, and the scatter tends to be gentler with time, likely due to the dissipation of residual heat to the surrounding soil. The linearity in the decay phase is comparatively lower than in the heating phase. It can also be observed that the slope in the decay phase is significantly higher (about ten times) than in the heating phase, indicating that temperature decay happens extremely fast.

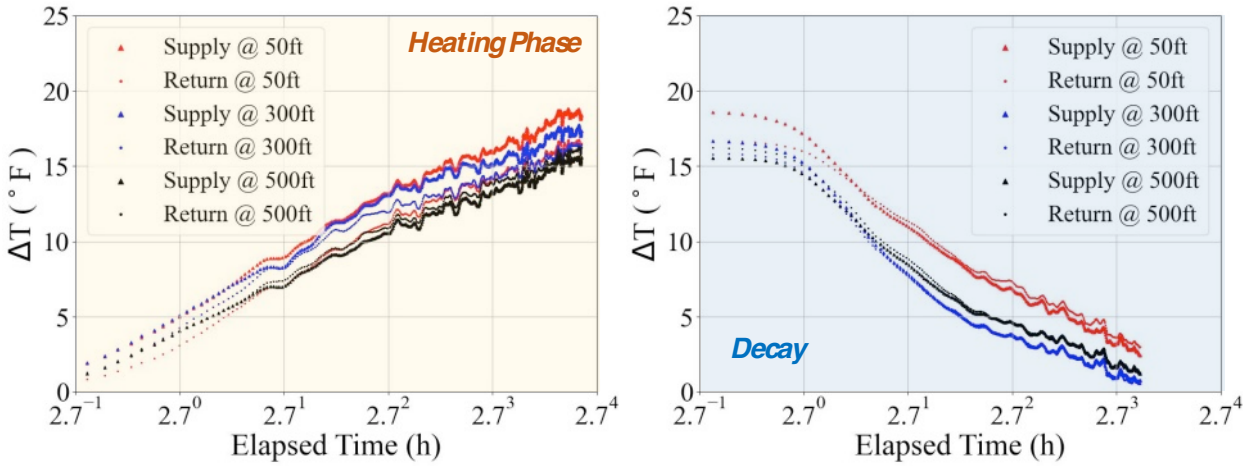

Figure 3–5 Comparison of the linearity of the temperature change (ΔT) time history in natural log time at selected depths during the heating and decay phase as recorded from the DFOS Outside instrumentation during the thermal response test conducted at the Farley Parking Lot geothermal borehole.

Table 3–2. Statistics on linear regression of temperature versus the natural log of time for stable regions during the heating (> 10 hr) and decay (> 1 hr) phase at selected depths recorded from the DFOS Outside instrumentation during the thermal response test conducted at the Farley Parking Lot geothermal borehole.

Depth (ft)	Heating Phase		Decay Phase	
	Slope	R^2	Slope	R^2
50	2.92	0.96	-22.36	0.84
300	2.36	0.93	-19.30	0.74
500	2.72	0.95	-19.53	0.77

3.1.2 Comparison with TRT Rig Data and Analysis

The water temperature measured at the surface with the TRT Rig thermocouples was processed (refer to Section 1.4 and Appendix B:) to obtain the thermal properties of the borehole. The geothermal properties from the GRTI TRT report (refer to Appendix C:) are summarized below.

- Ground Thermal conductivity: 1.78 Btu/hr-ft-°F
- Borehole Thermal Resistance: 0.245 hr-ft-°F/Btu
- Weighted average of heat capacity: 39.1 Btu/ft^3-°F
- Thermal diffusivity: 1.10 ft^3/day

Figure 3–6 compares the temperature measured near the ground surface using DFOS with the TRT Rig thermocouple sensors. Results show that the DFOS temperature is about 4 – 7 °F lower than TRT Rig thermocouple sensors. Since the outside instrumentation of DFOS measures ΔT in the grout, it is expected to be smaller than the water temperature measurement inside the U-Pipe.

The thermal conductivity (λ_g) was determined using Equation (1-3) by calculating the slope of temperature field T(t) against the natural logarithm of time (i.e., ln(t)) (see Figure 3–6). The slope is equal to $Q/4\pi\lambda_g$ for $\frac{\alpha_g t}{r_b^2} \geq 5$. The thermal conductivity estimated from the DFOS outside instrumentation was found to be 1.44 Btu/hr-ft-°F, lower than the 1.78 Btu/hr-ft-°F estimated from the TRT Rig temperature measurements. As expected, the thermal conductivity estimated using DFOS is smaller because the fiber optic cables were outside the U-Pipe in the grout. In contrast, the thermocouple sensor inside the TRT rig measured water temperature, where much of the applied heat dissipated.

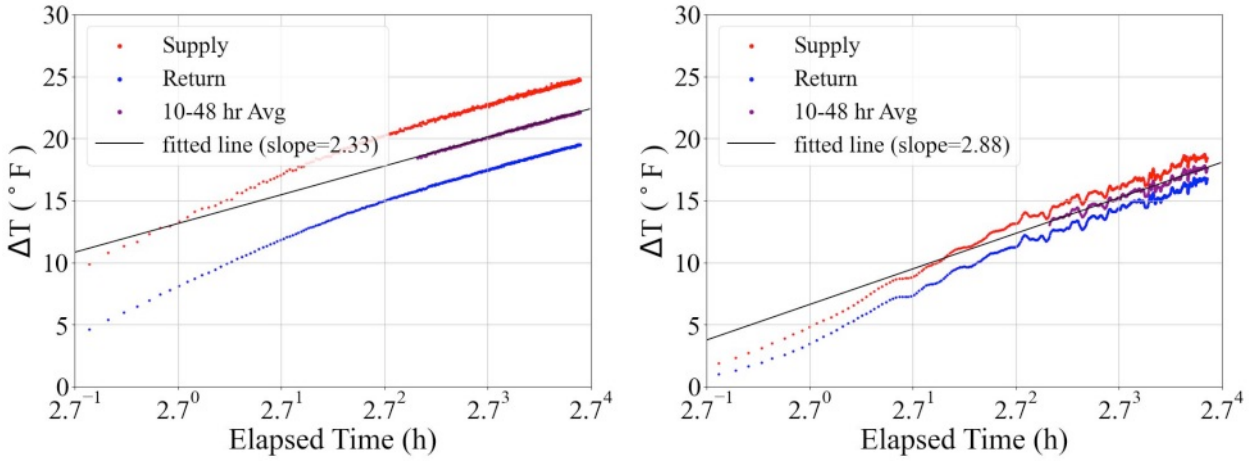

From thermocouple sensors (installed in TRT Rig) measuring fluid temperature

From DFOS outside instrumentation measuring fluid temperature

Figure 3–6 Comparison of temperature change (ΔT) measured near the surface using the thermocouple sensors installed in the TRT Rig with the DFOS Outside instrumentation (at about 50 ft) during the heating phase of the thermal response test conducted at the Farley Parking Lot geothermal borehole.

Using the outside DFOS instrumentation to estimate the ground thermal conductivity for estimating borehole thermal resistance requires advanced finite element analysis with modeling the heat exchange between the water-pipe-grout-soil interface. Alternatively, an inside DFOS instrumentation can directly measure the water temperature and can be used to estimate the ground thermal conductivity and borehole resistance. Section 3.4 describes the use of DFOS Inside instrumentation to measure geothermal borehole properties and the variation in thermal conductivity distribution with depth.

3.2 Rose Kennedy Geothermal Borehole

A TRT test was conducted on the Rose Kennedy borehole on Oct. 19 – 21, 2022. The full GRTI report describing the test statistics and analysis is provided in Appendix D:. Table 3–3 summarizes the test statistics.

The sampling rate was about 4 mins. The heating and decay phases were ~ 47 hours and 12 hours, respectively. Figure 3–7 shows the 2D contours of temperature change (ΔT) versus depth and time. To reduce noise and analyze the spatial-temporal characteristics, the raw ΔT data (Figure 3–7 (a)) were filtered using a 2D anisotropic Gaussian Filter with σ_{time} of 3 and σ_{depth} of 9 (Figure 3–7 (b)). The filtered data was used to analyze the temperature profile and time history at different depths and times, respectively.

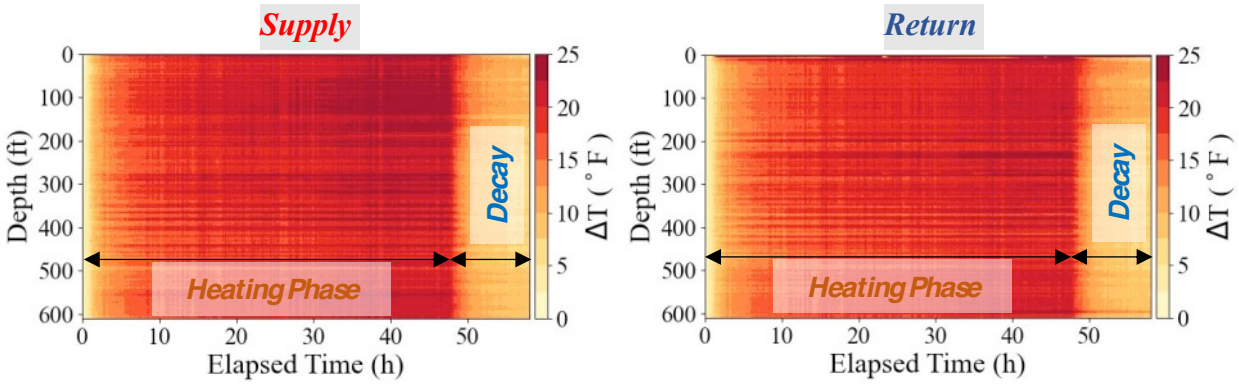

(a) Raw Data

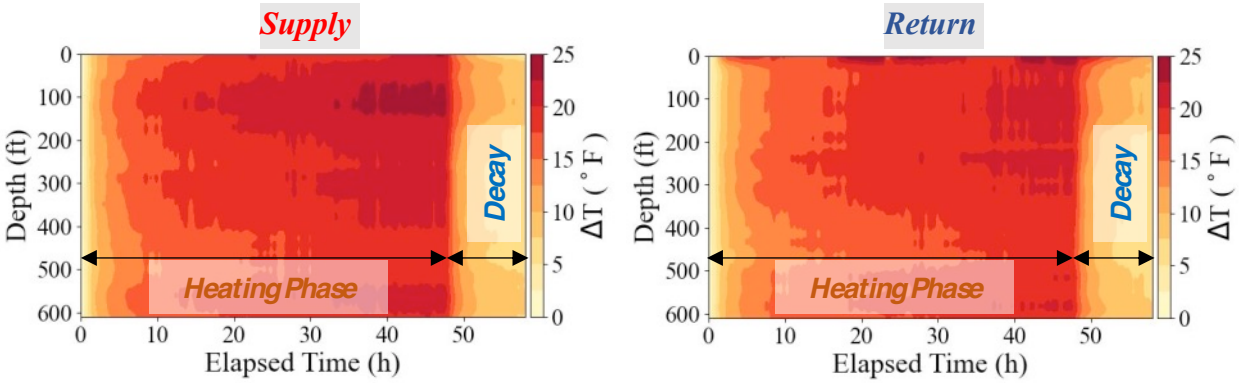

(b) Filtered Data

Figure 3–7 2D Contours of temperature change (ΔT) showing (a) raw and (b) filtered data with depth and time from the DFOS Outside instrumentation during the thermal response test conducted at the Rose Kennedy geothermal borehole.

Table 3–3. Thermal response test statistics for Rose Kennedy geothermal borehole.

Parameter	Values
Undistributed Formation Temperature	53.2 – 54.3 °F
Duration	47.0 hours
Average Voltage	238.8 V
Average Heat Input Rate	32118 Btu/hr (9411 W)
Average Heat Input Rate Density	52.7 Btu/hr-ft (15.4 W/ft)
Circulator Flow Rate	12.3 gpm
Standard Deviation of Power	0.09 %
Maximum Variation in Power	0.23 %

3.2.1 Time Histories and Profiles of Temperature Change (ΔT) Measurement

The filtered data was processed to investigate the temperature change (ΔT) time histories at selected depths. The ΔT time histories at selected depths of 50 ft, 200 ft, 300 ft, and 500 ft are shown in Figure 3–8. The total temperature increase near the surface (about 50 ft) was about 19 – 22 °F. As expected, the change in the supply temperature (ΔT_{supply}) is usually higher than ΔT_{return} (Figure 3–8). The total difference between ΔT_{supply} and ΔT_{return} near the surface was roughly 2 °F, which decreased with depth and ultimately converged to zero (at about 500 ft).

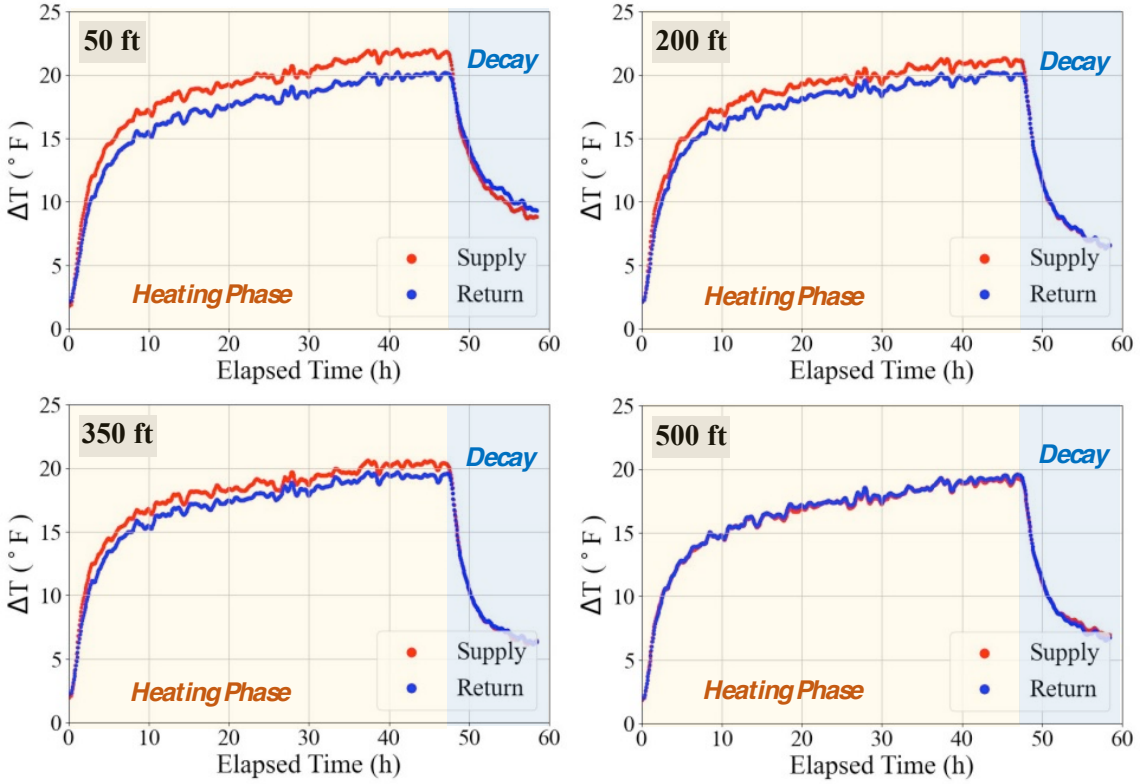

Figure 3–8 Recorded temperature change (ΔT) time-histories at selected depths from the DFOS Outside instrumentation during the thermal response test conducted at Rose Kennedy geothermal borehole.

The ΔT profiles at selected times during the heating and decay phase are shown in Figure 3–9. The figure shows that ΔT_{supply} is usually higher than ΔT_{return}, but the difference decreased with depth, leading to the formation of the "V" shape, as described in Section 1.4. Towards the end of the heating phase, ΔT at shallow depths increased by 20 – 24 °F, while at the bottom of the borehole, it only increased by 18 °F. Overall, the Rose Kennedy geothermal borehole's temperature increase was about 4 °F higher than the Farley Parking Lot geothermal borehole. During the decay phase, the difference between ΔT_{supply} and ΔT_{return} decreased quickly and ultimately converged over itself within a few hours, as shown in Figure 3–8 and Figure 3–9.

Like the Farley Parking Lot geothermal borehole, ΔT_{supply} and ΔT_{return} converged at a depth of 250 ft and below the depth of 500 ft, indicating that the heat transfer efficiency at these locations is low. Given that the borehole elevations in these two tests are very close (172.5 for the first and 202.5 for the second test), it might be caused by some geological conditions. Since the installation of the borehole was relatively good, the possible reason for any fluctuation in the temperature data could be the poor quality of grout or the geological conditions.

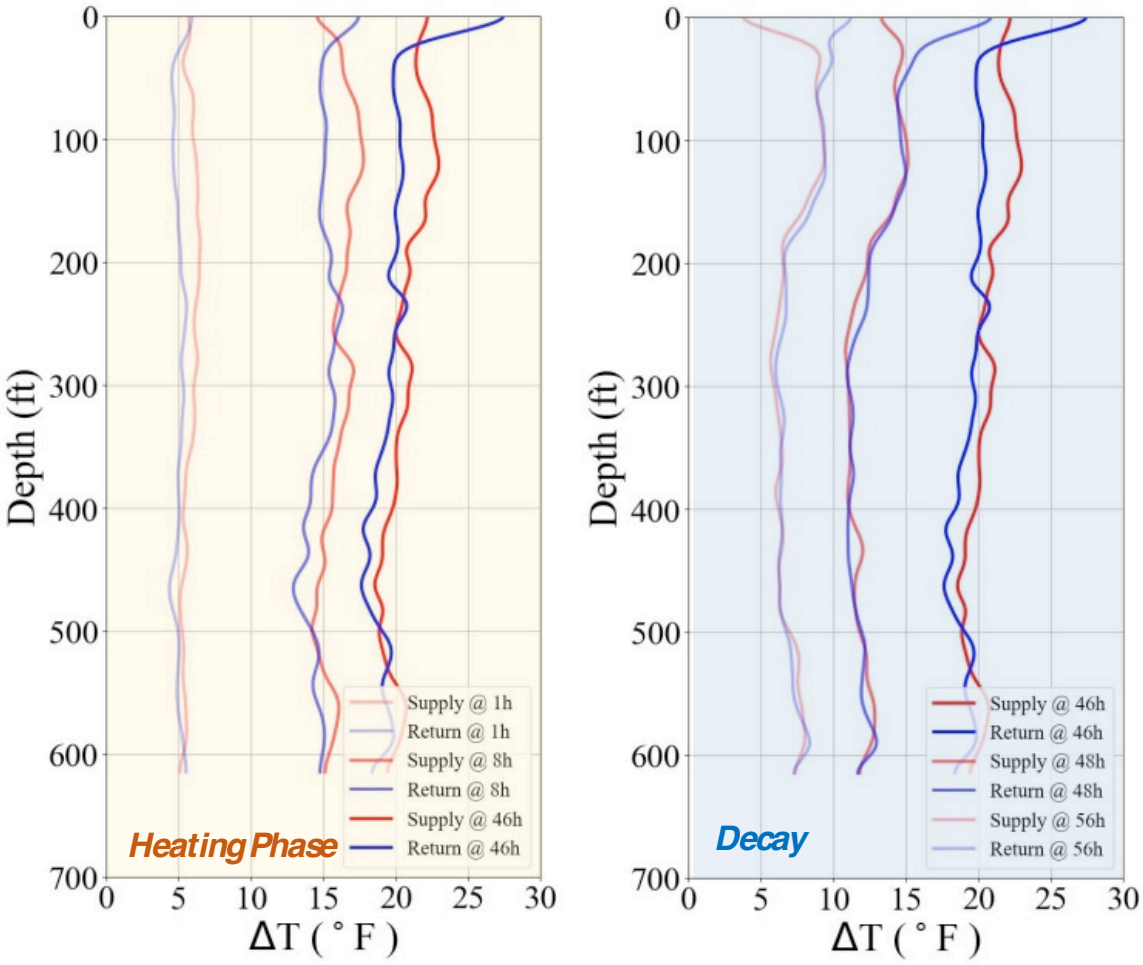

Figure 3–9 Profiles of temperature change (ΔT) at selected times during the heating and decay phase as recorded from the DFOS Outside instrumentation during the thermal response test conducted at the Rose Kennedy geothermal borehole.

Figure 3–10 investigates the linearity of ΔT time histories in natural log time at selected depths during the heating and decay phases. Table 3–4 summarizes the temperature data's linearity with the natural time log for the stable regions within the heating (> 10 hr) and decay (> 1 hr) phase. A strong linearity between ΔT and natural log time can be observed during the heating phase. However, the slopes are slightly different at different depths indicating the variable thermal conductivity with depth. For the decay phase (although the data is relatively short compared to the Farley Parking Lot geothermal borehole), it can still be found that the linearity decreases, and the scatter tends to be gentler with time, likely due to the dissipation of residual heat to the surrounding soil. Similar to the Farley Parking lot test, the linearity in the decay phase is comparatively lower than in the heating phase. On the other hand, the slope during the decay phase is significantly higher (about ten times) than during the heating phase, indicating that temperature decay happens extremely fast.

Table 3–4. Statistics on linear regression of temperature versus the natural log of time for stable regions during the heating (> 10 hr) and decay (> 1 hr) phase at selected depths recorded from the DFOS Outside instrumentation during the thermal response test conducted at the Rose Kennedy geothermal borehole.

Depth (ft)	Heating Phase		Decay Phase	
	Slope	R^2	Slope	R^2
50	3.05	0.96	-35.88	0.90
300	2.55	0.94	-34.47	0.84
500	2.82	0.96	-33.42	0.84

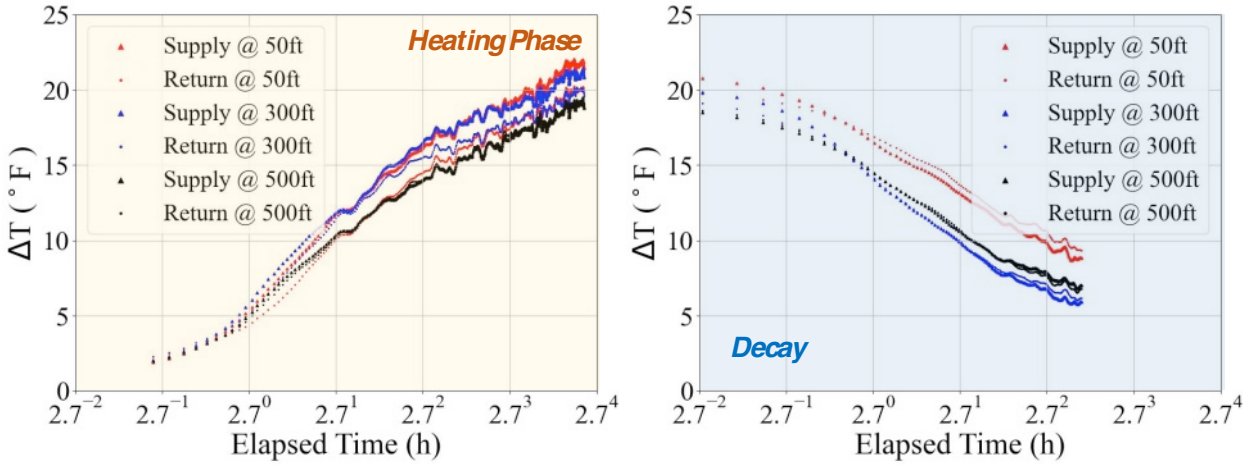

Figure 3–10 Comparison of the linearity of the temperature change (ΔT) time history in natural log time at selected depths during the heating and decay phase as recorded from the DFOS Outside instrumentation during the thermal response test conducted at the Rose Kennedy geothermal borehole.

3.2.2 Comparison with TRT Rig Data and Analysis

The water temperature measured at the surface with the TRT Rig thermocouples was processed (refer to Section 1.4 and Appendix B:) to obtain the thermal properties of the borehole. The geothermal properties from the GRTI TRT report (refer to Appendix D:) are summarized below.

- Ground Thermal conductivity: 1.57 Btu/hr-ft-°F
- Borehole Thermal Resistance: 0.241 hr-ft-°F/Btu
- Weighted average of heat capacity: 38.4 Btu/ft^3-°F
- Thermal diffusivity: 0.98 ft^3/day

Figure 3–11 compares the temperature measured near the ground surface using DFOS with the TRT Rig thermocouple sensors. Results show that the DFOS temperature is about 2 – 5 °F lower than TRT Rig thermocouple sensors. Since the outside instrumentation of DFOS measures ΔT in the grout, it is expected to be smaller than the water temperature inside the U-Pipe.

Like the Farley Parking Lot geothermal borehole, the thermal conductivity estimated from the DFOS outside instrumentation, 1.37 Btu/hr-ft-°F was lower than the 1.57 Btu/hr-ft-°F estimated from the TRT Rig temperature measurements. As expected, the thermal conductivity estimated using DFOS is smaller because the fiber optic cables were outside the U-Pipe in the grout. In contrast, the thermocouple sensor inside the TRT rig measured water temperature, where much of the applied heat dissipated. Section 3.4 describes the use of linear source theory on measurements from the inside instrumentation using DFOS for estimating geothermal borehole properties and variation thermal conductivity distribution with depth.

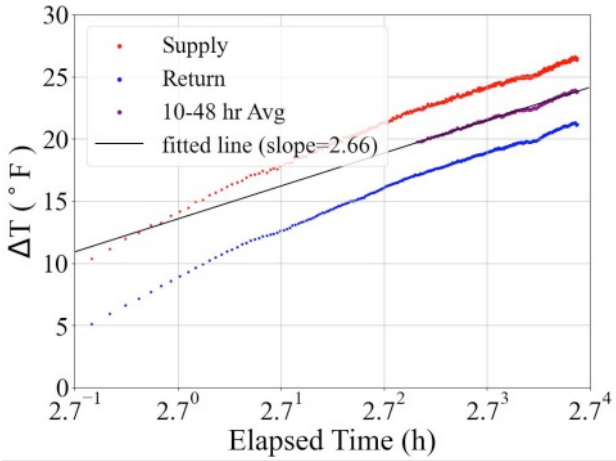

From thermocouple sensors (installed in TRT Rig) measuring fluid temperature

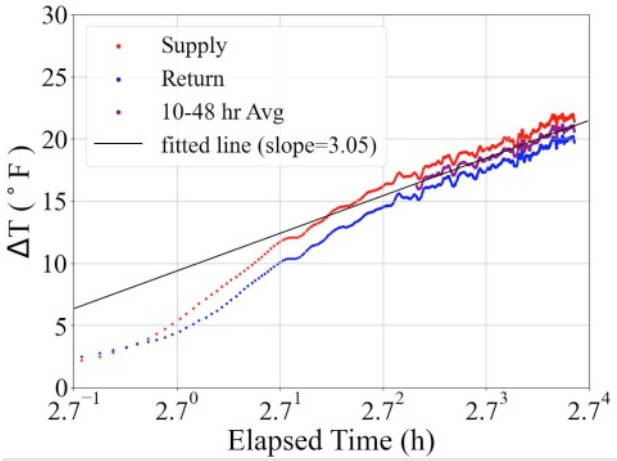

From DFOS outside instrumentation measuring fluid temperature

Figure 3–11 Comparison of temperature change (ΔT) measured near the surface using the thermocouple sensors installed in the TRT Rig with the DFOS Outside instrumentation (at about 50 ft) during the heating phase of the thermal response test conducted at the Rose Kennedy geothermal borehole.

3.3 Fire Station Geothermal Borehole

A TRT test was conducted on the Fire Station borehole on October 17 – 19, 2022, with both DFOS instrumentations: Inside and Outside, installed. The full GRTI report describing the test statistics and analysis is provided in Appendix E:. Table 3–5 summarizes the test statistics.

The sampling rate was about 3.5 mins. The heating and decay phases were ~ 47.4 hours and 4 hours, respectively. The temperature recording was interrupted between 15 – 25 hours due to the malfunctioning of the analyzer. Figure 3–12 and Figure 3–13 show the 2D contours of temperature change (ΔT) versus depth and time for the Outside and Inside instrumentation, respectively. To reduce noise and analyze the spatial-temporal characteristics, the raw ΔT data (Figure 3–12 (a), Figure 3–13 (a)) were filtered using a 2D anisotropic Gaussian Filter with σ_{time} of 3 and σ_{depth} of 9 (Figure 3–12 (b), Figure 3–13 (b)). The filtered data was used to analyze the temperature profile and time history at different depths and times, respectively.

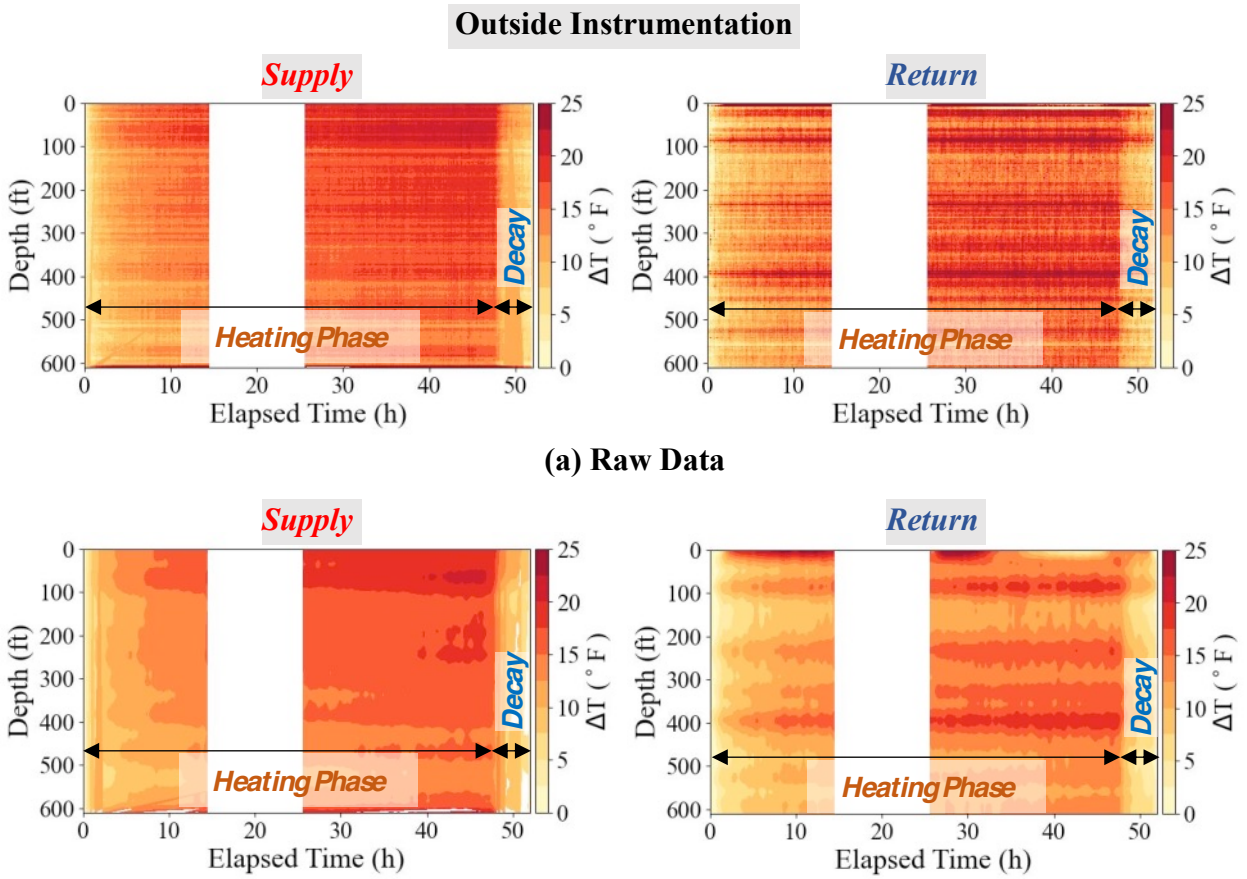

Figure 3–12 2D Contours of temperature change (ΔT) showing (a) raw and (b) filtered data with depth and time from the DFOS Outside instrumentation during the thermal response test conducted at the Fire Station geothermal borehole.

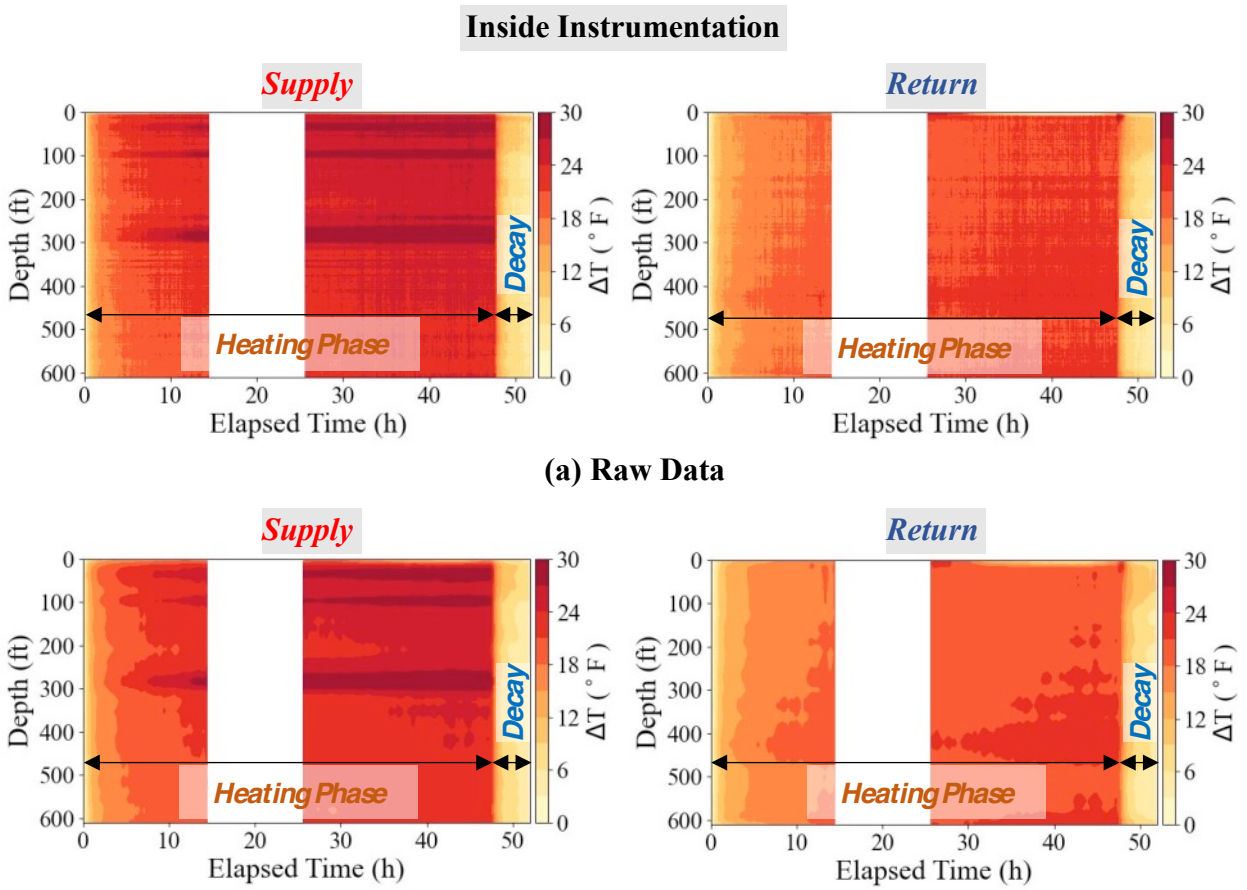

Figure 3–13 2D Contours of temperature change (ΔT) showing (a) raw and (b) filtered data with depth and time from the DFOS Inside instrumentation during the thermal response test conducted at the Fire Station geothermal borehole.

Table 3–5. Thermal response test statistics for Fire Station geothermal borehole.

Parameter	Values
Undistributed Formation Temperature	53.5 – 54.1 °F
Duration	47.4 hours
Average Voltage	238.8 V
Average Heat Input Rate	32082 Btu/hr (9400 W)
Average Heat Input Rate Density	52.6 Btu/hr-ft (15.4 W/ft)
Circulator Flow Rate	10.1 gpm
Standard Deviation of Power	0.04%
Maximum Variation in Power	0.11 %

3.3.1 Time Histories and Profiles of Temperature Change (ΔT) Measurement

The filtered data was processed to investigate the temperature change (ΔT) time histories at selected depths. The ΔT time histories at selected depths of 50 ft, 200 ft, 300 ft, and 500 ft from the Inside and Outside instrumentation are shown in Figure 3–14. The total temperature increases near the surface (about 50 ft) measured from the outside instrumentation was about 13 – 20 °F, and measured from the inside instrumentation was 20-28 °F. As expected, the ΔT is higher for the inside instrumentation, measuring the water temperature, than the outside instrumentation, which measured grout temperature. For the Outside instrumentation, the supply and return temperature converged at about 500 ft. In contrast, for the Inside instrumentation, they converged at the bottom of the borehole, i.e., at about 600 ft. For both cases, the supply temperature (ΔT_{supply}) is usually higher than ΔT_{return} (Figure 3–14) and decreases with depth. The measured total difference between ΔT_{supply} and ΔT_{return} near the surface from the Outside and Inside instrumentation was roughly 5 °F and 8 °F, respectively.

The filtered data was also processed to investigate the temperature change (ΔT) time histories at selected times during the heating and the decay phase. The ΔT profiles at selected times during the heating and decay phase for both the Inside and Outside instrumentation are shown in Figure 3–15. The figure shows that ΔT_{supply} is usually higher than ΔT_{return}, but the difference decreased with depth, leading to the formation of the "V" shape, as described in Section 1.4. The "V" shape curve is very prominent on the Inside instrumentation. The data from the Inside instrumentation is very good. The Outside instrumentation quality was bad (among the worst in all three tests), and hence severe fluctuation in temperature (ΔT) measurement can be seen. The twisting of the U-Pipe and the long length of the FO cable between the tape attachments leading to entanglement and non-uniform distance from the U-Pipe are likely reasons for the bad quality of the data.

Towards the end of the heating phase, ΔT in the grout (measured from the Outside instrumentation) at shallow depths increased by 12 – 19 °F, while at the bottom of the borehole, it only increased by 13 °F (Figure 3–15). This temperature change is very similar to the Farley Parking lot geothermal test. The profiles of ΔT from the Outside instrumentation illustrate convergence in ΔT_{supply} and ΔT_{return} at multiple depths such as 90 ft, 250 ft, and below the depth of 300 ft (Figure 3–15). The reason for so much convergence is likely due to the bad quality of the instrumentation. The supply and return FO cables are frequently too close to each other hence measuring similar temperatures. The inadequate instrumentation quality outweighs any fluctuations arising from the grouting quality or the variability in geological conditions.

For the Inside instrumentation (measuring the water temperature), at the end of the heating phase, the temperature at the shallow surface increased by 20 – 25 °F, whereas near the bottom of the borehole, it increased by 22 °F, much higher than the Outside instrumentation (Figure 3–15). ΔT_{supply} and ΔT_{return} converged below the depth of 550 ft. Spatial fluctuation is effectively relieved for the Inside instrumentation as the water temperature inside the U-Pipe at any depth is uniform and does not change with the radial distance within the small diameter of the pile. However, two sharp temperature spikes can be observed from the supply side at 40 ft and 280 ft, probably due to some non-linearity in the FO cable, which was corrected (refer to Section 3.4) by interpolating the data from the temperature measured closer to the affected depths.

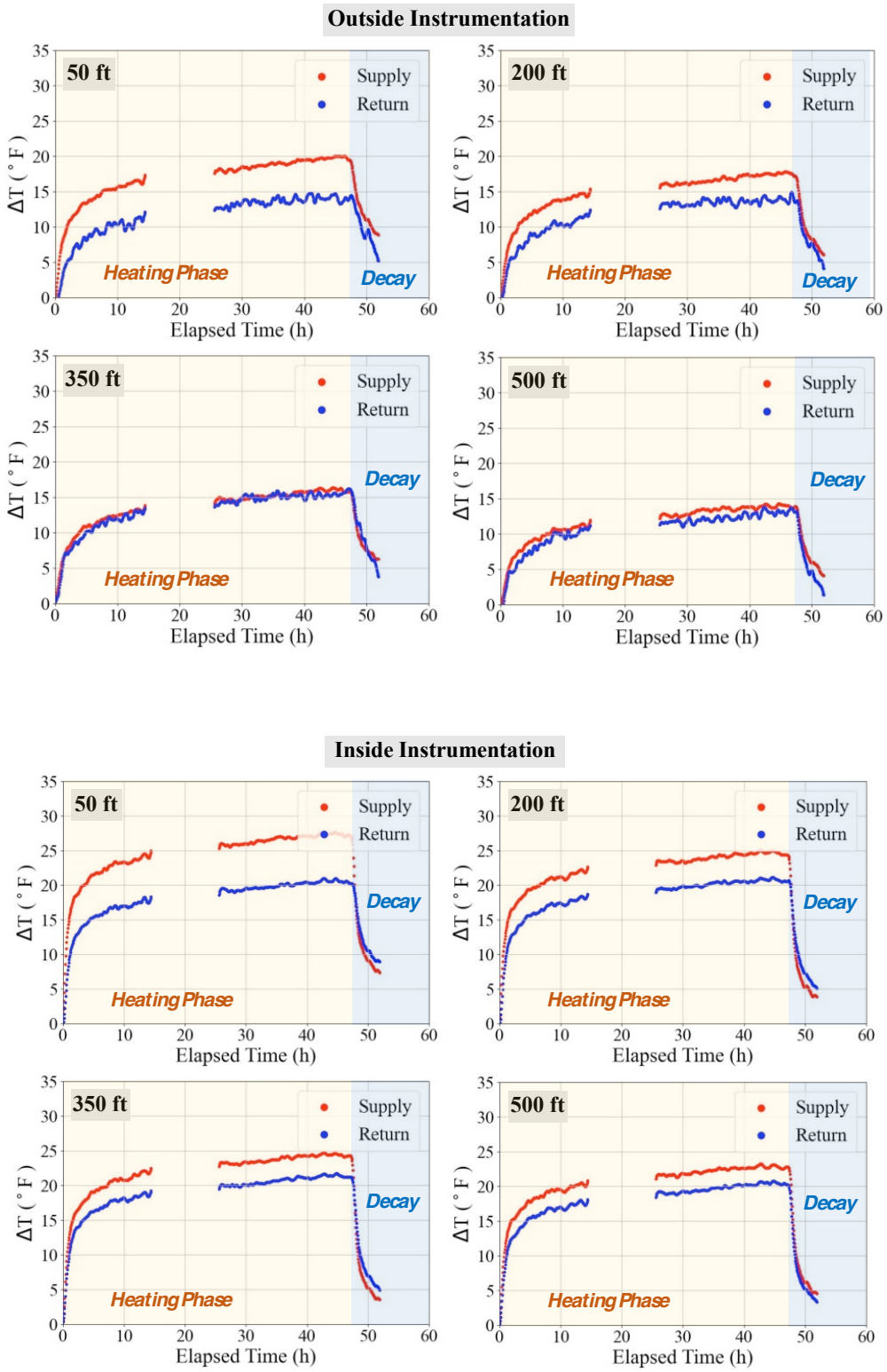

Figure 3–14 Recorded temperature change (ΔT) time-histories at selected depths from the DFOS Outside (top) and Inside (below) instrumentation during the thermal response test conducted at Fire Station geothermal borehole.

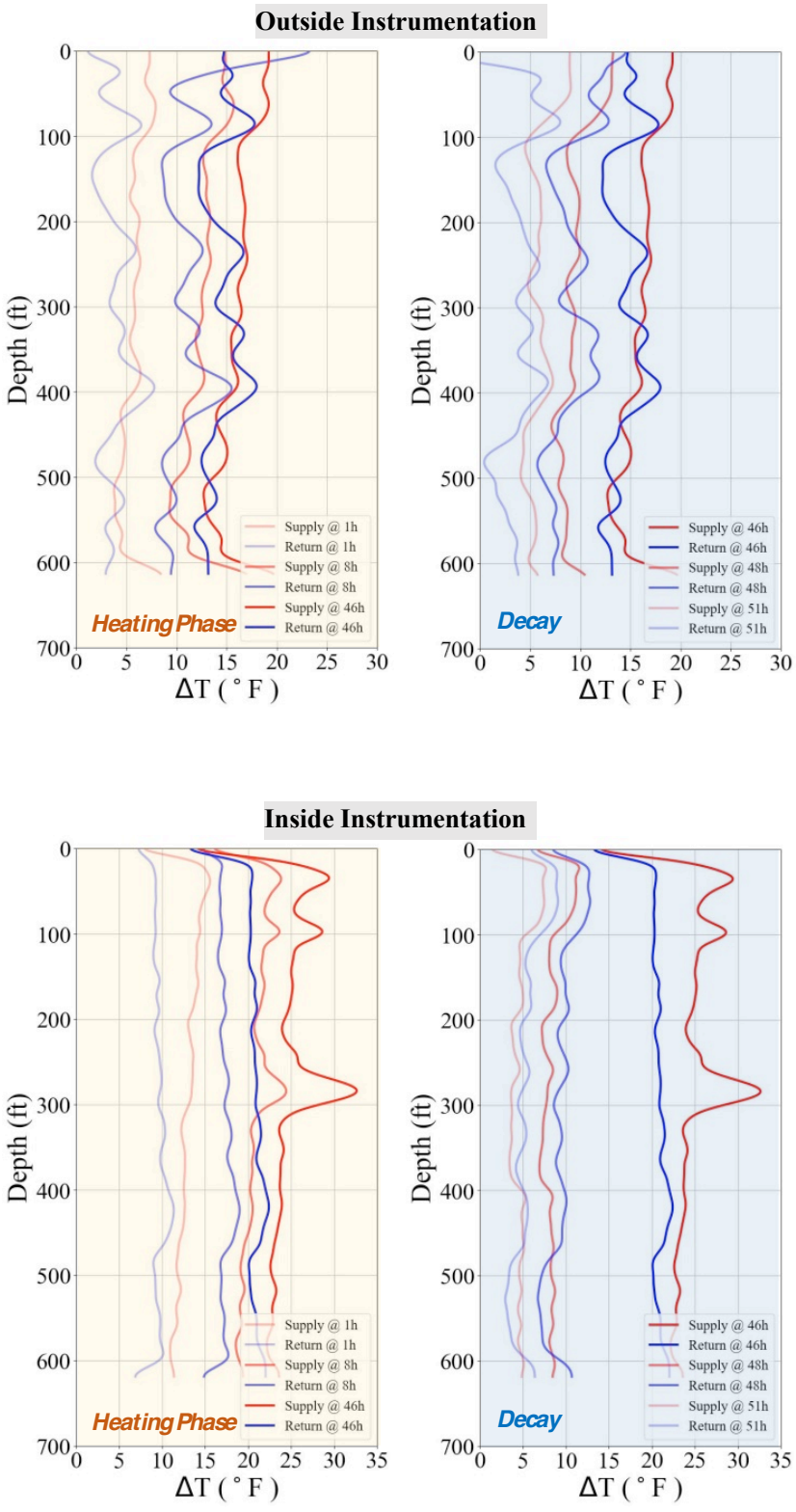

Figure 3–15 Profiles of temperature change (ΔT) at selected times during the heating and decay phase as recorded from the DFOS Outside (top) and Inside (below) instrumentation during the thermal response test conducted at the Fire Station geothermal borehole.

Figure 3–16 investigates the linearity of ΔT time histories in natural log time at selected depths during the heating and decay phases for both the Inside and Outside instrumentation. Table 3–6 summarizes the temperature data's linearity with the natural time log for the stable regions within the heating (> 10 hr) and decay (> 1 hr) phase. A strong linearity between ΔT and natural log time can be observed during the heating phase. However, the slopes are slightly different at different depths indicating the variable thermal conductivity with depth. In the decay phase, the linearity between ΔT and natural log time decreases, and the scatter tends to be gentler with time, likely due to the dissipation of residual heat to the surrounding soil. The slope during the decay phase at the Firestation site was obtained three times higher than the other TRT tests. Since the decay phase for the Firestation TRT test was relatively shorter (only about 4 hr), the slope analysis might have been heavily biased by the initial non-linear temperature data resulting in such large values.

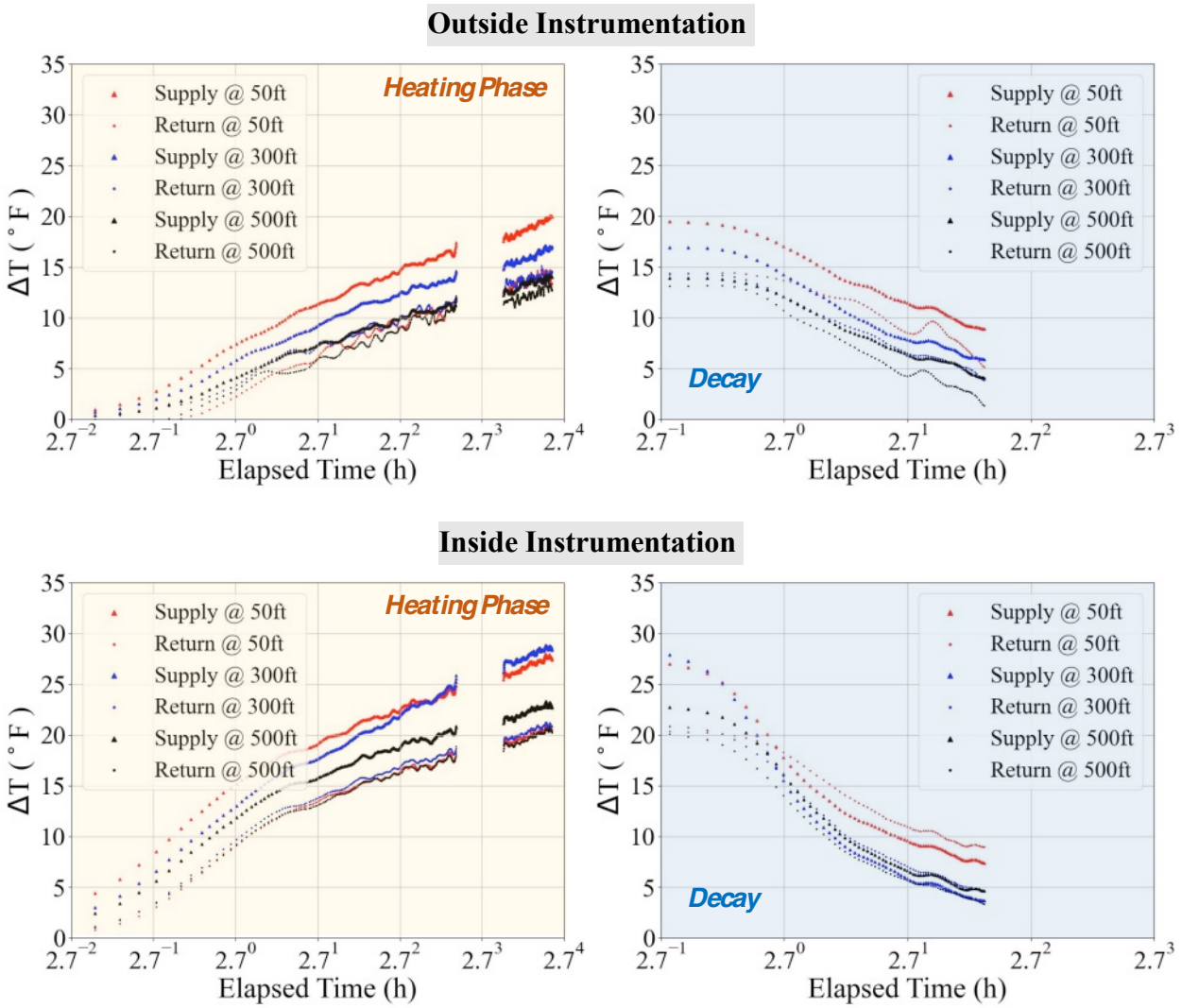

Figure 3–16 Comparison of the linearity of the temperature change (ΔT) time history in natural log time at selected depths during the heating and decay phase as recorded from the DFOS Outside (above) and Inside (below) instrumentation during the thermal response test conducted at the Fire Station geothermal borehole.

Table 3–6. Statistics on linear regression of temperature versus the natural log of time for stable regions during the heating (> 10 hr) and decay (> 1 hr) phase at selected depths recorded from the DFOS Outside and Inside instrumentation during the thermal response test conducted at the Firestation geothermal borehole.

Oustide Instrumentation

Depth (ft)	Heating Phase		Decay Phase	
	Slope	R^2	Slope	R^2
50	2.76	0.96	-88.34	0.94
300	2.46	0.97	-84.44	0.91
500	2.23	0.94	-87.39	0.91

Inside Instrumentation

Depth (ft)	Heating Phase		Decay Phase	
	Slope	R^2	Slope	R^2
50	2.64	0.97	-96.94	0.86
300	2.88	0.98	-107.00	0.84
500	2.34	0.96	-101.00	0.83

3.3.2 Comparison with TRT Rig Data and Analysis

The water temperature measured at the surface with the TRT Rig thermocouples was processed (refer to Section 1.4 and Appendix B:) to obtain the thermal properties of the borehole. The geothermal properties from the GRTI TRT report (refer to Appendix C:) are summarized below.

- Ground Thermal conductivity: 1.92 Btu/hr-ft-°F
- Borehole Thermal Resistance: 0.236 hr-ft-°F/Btu
- Weighted average of heat capacity: 36.1 Btu/ft^3-°F
- Thermal diffusivity: 1.28 ft^3/day

Figure 3–17 compares the temperature measured near the ground surface using DFOS with the TRT Rig thermocouple sensors. Similar to the previous tests, results show that the DFOS temperature measured from the Outside instrumentation is about 3 – 5 °F lower than TRT Rig thermocouple sensors. Since the outside instrumentation of DFOS measures ΔT in the grout, it is expected to be smaller than the water temperature measurement inside the U-Pipe. As a result, the thermal conductivity estimated from the DFOS outside instrumentation is 1.52 Btu/hr-ft-°F, lower than the 1.92 Btu/hr-ft-°F estimated from the TRT Rig temperature measurements.

On the other hand, the DFOS temperature (of the water) measured from the Inside instrumentation matches quite well with the TRT Rig thermocouple sensors, thus validating the

temperature measurements. Consequently, the estimated thermal conductivity of 1.71 Btu/hr-ft-°F obtained from the DFOS Inside instrumentation matches better with the 1.92 Btu/hr-ft-°F estimated from the TRT Rig temperature measurements.

Results show that the DFOS Inside instrumentation can directly measure the water temperature and can be used to estimate the ground thermal conductivity and borehole resistance. On the other hand, using the outside DFOS instrumentation to estimate the ground thermal conductivity requires advanced numerical analysis involving modeling the heat exchange between the water-pipe-grout-soil interface. The following section uses the data from the Inside instrumentation to estimate variability in the thermal conductivity of the borehole with depth.

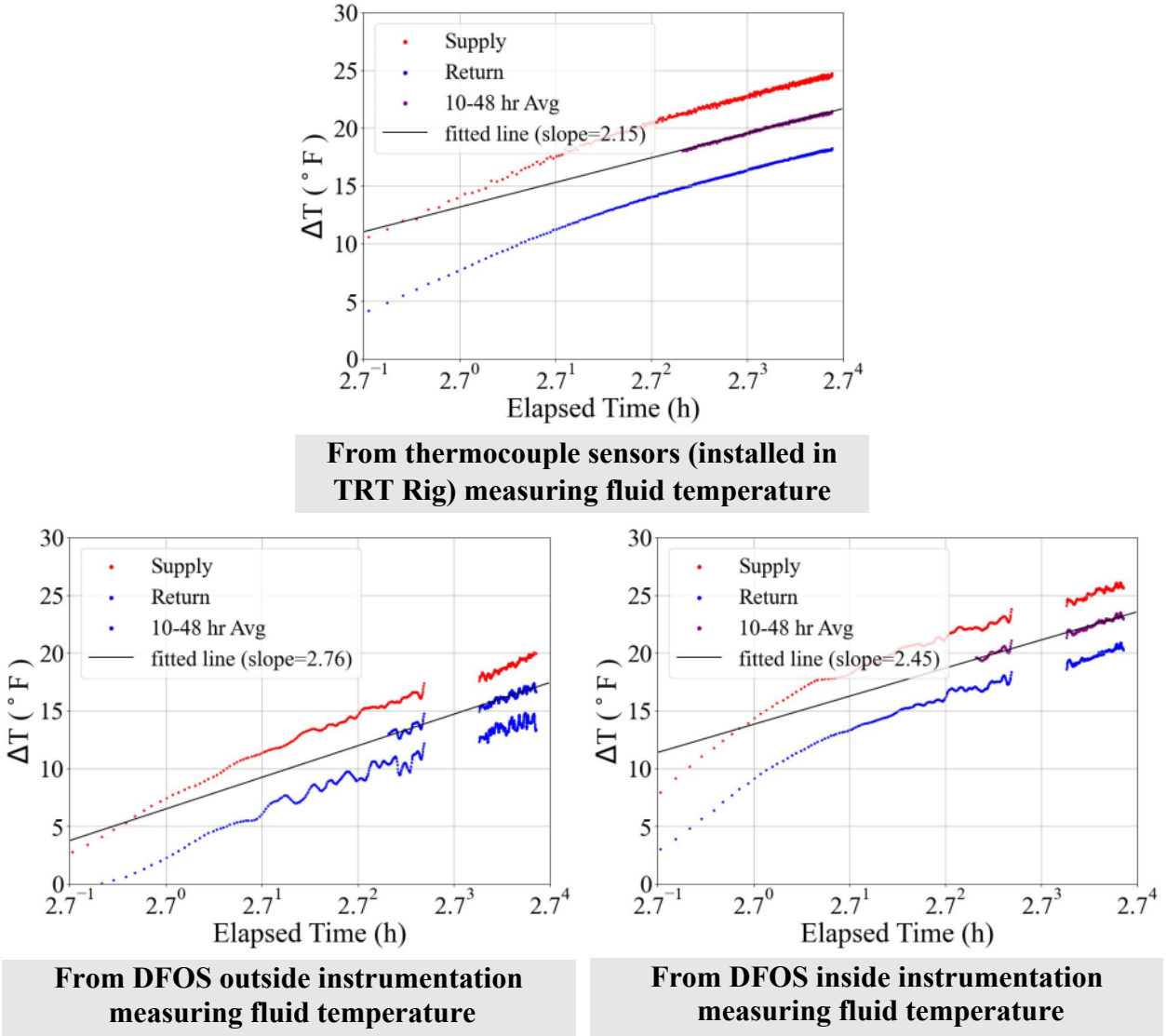

Figure 3–17 Comparison of temperature change (ΔT) measured near the surface using the thermocouple sensors installed in the TRT Rig with the DFOS Outside and Inside instrumentation (at about 50 ft) during the heating phase of the thermal response test conducted at the Fire Station geothermal borehole.

3.4 Thermal Conductivity Profile using DFOS Inside Instrumentation Data

The most common way of estimating thermal conductivity, i.e., the line source method (using the average supply and return temperature at the surface), ignores the vertical heat transfer and any variability of the thermal conductivity in the soil layers. Temperature profile data from DFOS provided the capability and potential to obtain the variation in thermal conductivity with depth, which can help better understand the heat exchange within the ground, thus enabling more efficient design.

To extract the vertical distribution of thermal conductivity from the DFOS Inside Instrumentation data, the analytical method developed by McDaniel et al. (2018), following the work of Molz et al. (1989), was applied in this study. The method assumes the radial temperature gradients from the U-tube to the subsurface are constant and uniform at the steady state. The thermal conductivity values at different depths can be calculated from the temperature gradient and total average thermal conductivity when the test reaches a steady state. The equations used in the method are as follows:

$$\frac{\lambda_i}{\lambda_g} = \frac{\frac{\Delta Q_{H,i}}{\Delta z_i}}{QP_H/B} \quad \textbf{(3-1)}$$

$$\Delta Q_{H,i} = \Delta T * Q_w * \rho_w * c_{p,w} \quad \textbf{(3-2)}$$

where

λ_i is the thermal conductivity of the ith layer

λ_g is the total average thermal conductivity from traditional TRT

$\Delta Q_{H,i}$ is the incremental heat flow

QP_H is the sum of $\Delta Q_{H,i}$

Δz_i is the thickness of the ith layer

B is the depth of the borehole

Q_w is the flow rate

ρ_w is the density of water, and

$c_{p,w}$ is the heat capacity of water.

3.4.1 Results from the DFOS Inside Instrumentation at the Fire Station Borehole

The methodology described above can be used only with the inside instrumentation. Thus, it was used only at the Fire Station borehole where inside instrumentation was performed. The subsurface was first divided into several layers based on the recorded temperature change profile (Figure 3–18). For each layer, straight lines were used to represent the temperature change (ΔT) in the supply and return sides. Since several anomalies existed in the temperature of the supply

side among depths of 25 – 60 ft, 85 – 110 ft, and 260 – 310 ft, data in these sections were removed and linearly interpolated from the neighboring data. Although this method can be vulnerable to temperature fluctuation, it can still provide a decent estimate of the thermal conductivity profile. The profile at 46 hours was chosen as the temperature of the steady state. Figure 3–18 shows the simplified temperature profile, temperature gradient, and thermal conductivity. The thermal conductivity (λ) for the sediment layer above 60 ft was found to be 2.3 Btu/hr-ft-°F, which then increased to 3.8 Btu/hr-ft-°F at the interface of sediment and bedrock. The bedrock's thermal conductivity (λ) within the depth of 90 – 260 ft was found to be 0.9 Btu/hr-ft-°F and 2.1 – 2.3 Btu/hr-ft-°F below 260 ft.

Compared with conventional TRT, the data from the DFOS helped identify the low thermal conductivity zone between the depth of 85 – 260 ft. The results show that designing boreholes with lengths smaller than 260 ft at the test site will result in lower heat transfer efficiency.

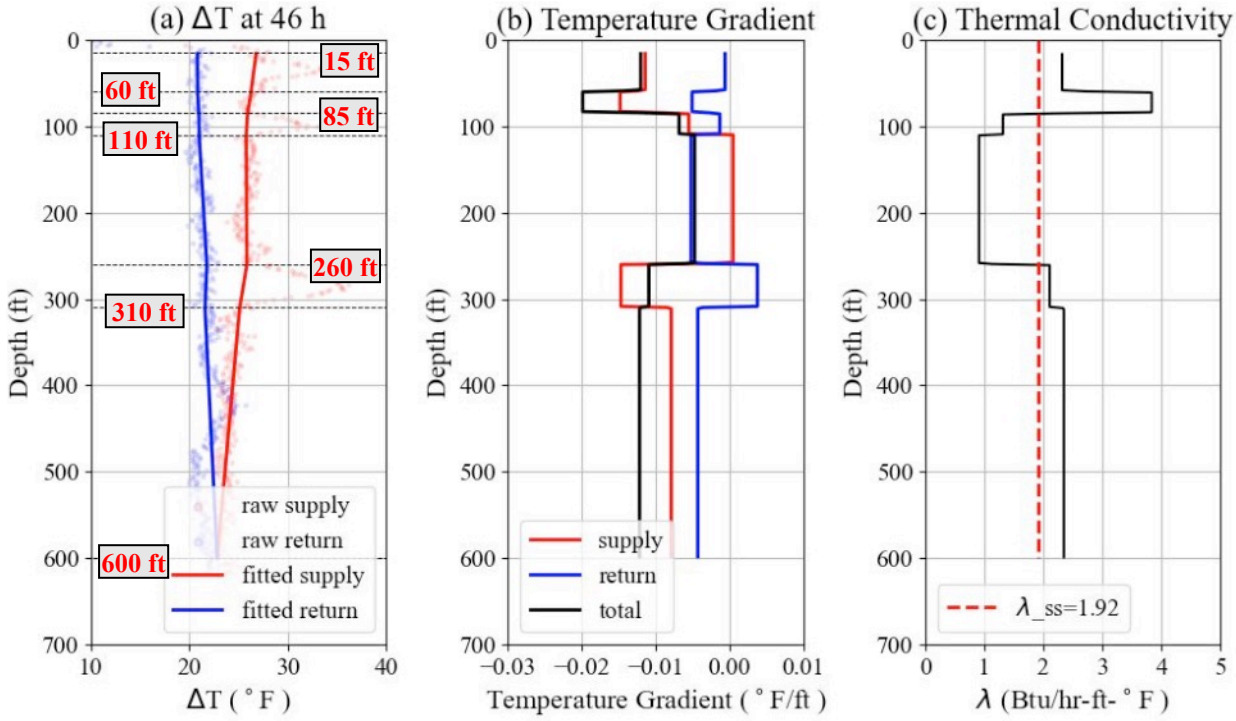

Figure 3–18 Calculating the thermal conductivity profile using the Inside Instrumentation at the Fire Station geothermal borehole.

The heat capacity profile at the test site was estimated based on the typical heat capacity values of soils/rocks listed by Kavanaugh and Rafferty (2014). As shown in Table 3–7, the ground was divided into two primary layers (see Table 2–1), and a range of heat capacity was estimated for each layer. The thermal diffusivity profile was obtained by combining the heat capacity with the thermal conductivity profile, which is shown in Figure 3–19. Results show that the thermal diffusivity for the sediment layer (above 85 ft) is 1.2 – 4.6 ft^2/day. For the bedrock layer, the thermal diffusivity is 0.5 – 0.7 ft^2/day between 85 – 260 ft depths, which increases to 1.2 – 1.7 ft^2/day to the depth below it.

Table 3–7. Summary of the layered heat capacities at the Fire Station geothermal borehole.

Layer	Description	From (ft)	To (ft)	Heat Capacity (Btu/ft^3-°F)	
				Lower Bound	Upper Bound
1	Overburden (brown cobbles, fine sand)	0	84	20.2	43.0
2	Grey Diorite, Gabbro	84	610	33.9	48

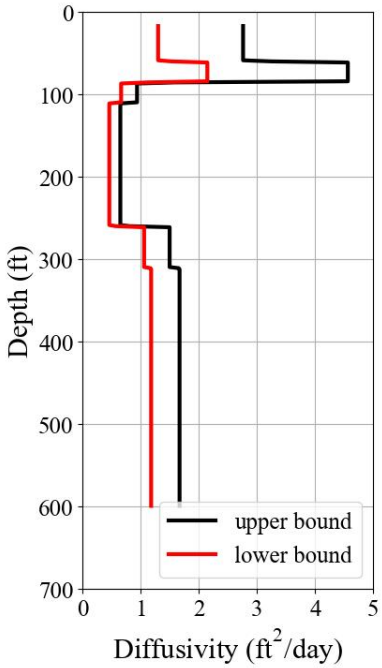

Figure 3–19 Thermal diffusivity profile at the Fire Station geothermal borehole.

4 SUMMARY AND CONCLUSIONS

4.1 Summary

This report described the installation, testing, and analysis of temperature measurements using distributed fiber optic sensing (DFOS) during the thermal response tests conducted on geothermal boreholes at three locations in Framingham, MA. The tests were conducted as a part of the pilot project investigating the design and development of "Networked Geothermal," an innovative green technology that has the potential to provide the heating and cooling needs of residential homes in a safe, non-emitting, and affordable way, thus reducing our dependence on the natural gas. The initiative falls under the Massachusetts 2050 Decarbonization Roadmap, which mandates net zero greenhouse gas (GHG) emissions by 2050. The three testing locations were (1) Framingham Fire Station, (2) Farley Parking Lot, and (3) Rose Kennedy, all in Framingham, MA. Different installation methods using DFOS were investigated, and their effect on the quality of data obtained was evaluated. The data obtained from the DFOS was analyzed to understand the thermal response of the geothermal borehole.

Each geothermal borehole was about 600 feet deep and consisted of one U-loop having one supply and a return pipe. Fiber optic cables were installed inside and outside the U-loop to monitor changes in the temperature of the circulating fluid (inside the U-Pipe) and the grout (outside the U-pipe). The data obtained using DFOS technology had a spatial resolution of 1 m and a temporal resolution of about 4 minutes. An industry-standard thermal response test (TRT) was conducted, where a constant input heat was applied for about 48 hours (referred to as a 'heating phase') with continuous water circulation. After its completion, the input heat and water circulation were stopped. The DFOS continuously took measurements while the water temperature decayed to the surrounding (referred to as the 'decay phase'). The data from the DFOS instrumentation recorded during the TRT test was processed and analyzed to increase the understanding of the boreholes' thermal response and their properties. Finally, the results from these initial geothermal boreholes tested under the pilot testing program were used to evaluate the effectiveness of the DFOS technology on geothermal boreholes laying out some important conclusions and recommendations for future work, as outlined in the sub-sections below.

4.2 Conclusions

Outlined below are some important conclusions regarding the use of DFOS technology in geothermal boreholes.

- Using DFOS technology on geothermal boreholes can provide time histories of temperature change and its distribution throughout the depth of the borehole at fine spatial and temporal resolution. Analyzing the temperature change distribution with depth can significantly increase our understanding of the thermal properties of the soil layers, which can aid in better and more efficient design.
- Fiber optic cables (FO) can be installed outside and inside the U-Pipe. The Outside instrumentation measures the temperature change in the grout, whereas the Inside instrumentation measures the water temperature circulating in the U-Pipe. The temperature

change occurring inside and outside the U-Pipe can be used to understand the heat exchange between the water-pipe-gout-soil interface.

- Temperature measurement from the Outside instrumentation was found sensitive to the position of the FO cable relative to the U-Pipe. Results show that frequent attachments of the FO cable to the U-Pipe at every 1 m ensures a uniform position of the cable to the U-Pipe. Additionally, twisting of the U-Pipe, entanglement of the FO cable due to large spacing between successive tape attachments, variability in geological materials, and grout quality can also result in spatial fluctuations in temperature measurements and make interpretation difficult.
- An innovative solution for the Inside instrumentation was proposed where the two cores of the FO cables were spliced together and inserted inside the U-Pipe. The advantage of such instrumentation is that the FO cables from both the Inside and Outside can be spliced together into just one cable. Having only one cable where both ends are accessible makes data collection possible using Brillouin Optical Time Domain Analysis (BOTDA) technology which has a better resolution. Also, having all cables connected to one makes instrumentation easier and reduces time in post-processing. The inside instrumentation measuring water temperature did not suffer from spatial fluctuations in temperature measurements.
- Results from the DFOS instrumentation during the heating phase clearly showed the "V" shaped curve between the supply and return pipes. The temperature change between the supply and the return pipes was largest at the surface and decreased with depth. As expected, the temperature in the grout was measured lower than the water temperature at all depths. Consequently, the thermal conductivity estimated from the Outside instrumentation was lower than the Inside instrumentation.
- During the decay phase, the temperature decreases rapidly with time. Within a few hours, the temperature of the supply and return sides of the U-Pipe converges and then continues to decrease further.
- Temperature measurement during the heating phase at the surface from the Inside instrumentation (and correspondingly the associated thermal conductivity) matched decently with the thermocouple sensors installed in the TRT rig, thus validating the measurements of DFOS. Analyzing the temperature profile obtained from the DFOS Inside instrumentation provided an estimation of the variation of thermal conductivity with depth.

4.3 Recommendations

The sub-sections below describe recommendations for future installation, testing, and analysis.

4.3.1 Installation

- It is essential to have good quality Outside instrumentation to prevent any spatial fluctuations in the recorded temperature measurement. Good quality outside instrumentation refers to a uniform fiber optic (FO) cable position relative to the U-pipe. A few recommendations include

    - Having frequent attachments of the FO cable with the U-Pipe (no more than 3 feet) ensures it always remains in contact. It could be challenging, especially when the U-Pipe is inserted into the ground, especially if the operator does not have the proper equipment to halt the insertion at regular intervals. Alternatively, the FO cables can be attached to the U-Pipe either during fabrication or in advance before installing in the borehole.
    - Care should be taken to ensure the FO cables remain on the same side of the U-Pipe (either on the supply or the return side) if some twisting occurs as it is inserted in the borehole.
- Care should be taken to reduce regions of optical loss in instrumentation. Loss of optical signal results in poor data quality. The leading cause of optical loss in the pilot test was the small diameter turns at the bottom of the U-Pipe for both the Outside and Inside instrumentation.
- It is essential to have a sufficient FO cable length (at least 20 feet) from the connection to the analyzer to the beginning of the sensing location. A considerable cable length is required so that the strength of any reflection from the connection dies down before it reaches the location where the measurement needs to be taken.

4.3.2 Testing

- For long-term and continuous monitoring, the analyzer should have capabilities such as remote access, an automatic alarm system, and the ability to transmit data over the cloud.
- The decay phase can take several days before the temperature of the U-Pipe and the grout return to the ambient conditions. It would be worthwhile to investigate if the rate of decay can be decreased by continuing the circulation like during the heating phase.

4.3.3 Analysis

While several methods exist for estimating thermal properties of the borehole, they are all based on the temperature measurement of the water inside the pipe. Future research needs to be performed on developing methods to estimate thermal properties using the temperature data of the grout/soil outside the pipe. Advanced finite element analysis which models the heat exchange between the grout, pipe, and water can help in an increased understanding of the thermal response of geothermal boreholes. Similarly, analysis methods should also be developed on using the decay curves for estimating thermal properties of the borehole.

5 REFERENCES

Gehlin, S. (2002). “Thermal Response Test - Method Development and Evaluation.” LULEA University of Technology.

HEET. (2017). *Geo Micro District: Feasibility Study*. Boston, Massachusetts.

Hu, D. J. J., Humbert, G., Dong, H., Zhang, H., Hao, J., and Sun, Q. (2021). “Review of specialty fiber-based Brillouin optical time domain analysis technology.” *Photonics*, 8(10).

Ismay, D., Miller, B., Chu, H.-H., Miziolek, C., Walsh, M., Edington, A., Hanson, L., Perry, D., and Laurent, C. (2020). *Massachusetts 2050 Decarbonization Roadmap*. Boston, Massachusetts.

Kavanaugh, S., and Rafferty, K. (2014). *Geothermal Heating and Cooling: Design of Ground-Source Heat Pump Systems*. ASHRAE, Atlanta, GA.

McDaniel, A., Tinjum, J., Hart, D. J., Lin, Y. F., Stumpf, A., and Thomas, L. (2018). “Distributed thermal response test to analyze thermal properties in heterogeneous lithology.” *Geothermics*, Elsevier, 76(September 2017), 116–124.

Molz, F. J., Morin, R. H., Hess, A. E., Melville, J. G., and Guven, O. (1989). “The Impeller Meter for Measuring Aquifer Permeability Variations’ Evaluation and Comparison With Other Tests.” *Water Resources Research*, 25(7), 1677–1683.

APPENDIX

APPENDIX A: DESCRIPTION OF GEOLOGICAL MATERIALS

APPENDIX C – DESCRIPTION OF GEOLOGIC MATERIALS BENEATH SCREENING LEVEL 2 SITES

A detailed assessment of the surficial geology and bedrock conditions beneath each of the sites that made it to Screening Level 2 is presented in this Appendix C. Source information for this assessment was obtained from available published mapping of the Massachusetts Geological Survey (MGS) and the U.S. Geological Survey (USGS), the Massachusetts Department of Environmental Protection (MassDEP) well records database, logs for geothermal test holes drilled at certain sites, consult with a local drilling company, and the combined experiences of the CDM Smith team. The findings of this assessment are presented below.

C.1 – DESCRIPTION OF SURFICIAL GEOLOGIC MATERIALS

Descriptions of the types of surficial geologic materials found beneath the Screening Level 2 sites are below. "Surficial materials" are defined as unconcolidated (or non-cemented, non-lithified) granular deposits that are either loose, such as beach sand, or can be crumbled using ones hand or a shovel, and occur from land surface downwards to bedrock. The surficial materials are distinguished from the bedrock formations that occur beneath the Screening Level 2 sites, which have many origins (including once an unconsolidated material) and have become crystallized or otherwise hardened deep underground **("metamorphosed")** over long periods of time as the materials were subjected to high temperatures and pressures.

C.1.1 - Recent Deposits (Postglacial)

Artificial fill is earth and manmade materials that have been artificially emplaced, typically in highway and railroad embankments, urban-development areas, and filled coastal wetlands.

Flood-plain alluvium is comprised of interlayered sand, gravel, silt, and organic material deposited beneath the flood plains of modern streams. Along smaller streams, alluvium is commonly less than 5 feet (ft) thick and typically covers older glacial stratified deposits.

Swamp deposits consist of organic muck and peat that can contain small amounts of sand, silt, and clay. They occur in swamps and freshwater marshes, in depressions in the land surface leftover from the glacial era, and in poorly drained areas. Where shown on the maps, they are inferred to be at least 3 ft thick. Most swamp deposits are less than 10 ft thick, and they overlie older glacial deposits or bedrock.

C.1.2 - Glacial Stratified (Layered) Deposits

Glacial stratified deposits that occur at the sites are distinguished by the size of the grains (particles) of the earth materials, specifically there are *coarse deposits* and *fine deposits*.

Coarse deposits consist of predominantly sand, gravel, or a mixture of sand and gravel as described below.

1

- *Sand deposits* are commonly interlayered with each layer having sand with a uniform grain **size ("well sorted"). These deposits can also be mixed with gravel (up to 25 percent gravel** particles) or some very fine sand, silt, and clay.
- *Gravel deposits* are composed of at least 50 percent gravel-sized particles, and may contain smaller amounts of cobbles, boulders, and sand mixed with the gravel and as separate **layers. Gravel layers typically have particles in a wide range of sizes ("poorly sorted").**
- *Sand and gravel deposits* occur as mixtures of gravel and sand within individual layers and as layers of sand alternating with layers of gravel. The proportion of sand to gravel generally ranges between 25 and 50 percent gravel particles and between 50 and 75 percent sand particles. Individual layers are well sorted to poorly sorted.

Glaciomarine fine deposits include a mix of clay, silty clay, fine sand, and some fine gravel deposited in lakes, marine environments along the coast and/or in tidal river estuaries. These materials range in thickness generally from a few feet to 75 ft.

C.1.3 - Glacial Till Deposits

Two types of glacial till occur at the sites, generally distinguished by thickness and how it was deposited by the glaciers.

Thin till is generally less than 10 to 15 ft thick and forms a layer over the top of the bedrock throughout much of the area. Thin till is mapped to occur at the surface where bedrock lies at a shallow depth. This till was deposited beneath the glacier **("lodgement" till) or near the glacier as it melted ("ablation" till). Both types of thin till** are a poorly sorted mix of sand, silt, clay with occasional gravels, cobbles, and boulders. The lodgement till is more compact as it was compressed under the weight of the glacier, while the ablation till is loose to moderately compact.

Thick till is greater than 10 to 15 ft thick and can be greater than 100 ft thick (the maximum recorded thickness in eastern Massachusetts is 230 ft). The shallow portion of thick till deposits consists of a poorly-sorted mix of sand, silt, clay with occasional gravels, cobbles, and boulders, like the thin till. At greater depths, the till is more like a lodgement till; it becomes compact and finer grained, i.e., contains a greater proportion of silt, very fine sand, and some clay. Thick till occurs in the form of **"drumlins,"** which are oval-shaped mounds of glacial till formed under the weight of a moving glacier and elongated in the direction of flow of the glacier. Drumlins often form over a high point, or knob, on the bedrock surface.

C.1.4 - Bedrock Areas

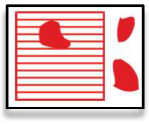

Bedrock Areas are areas where bedrock is exposed at the surface ("outcrops") over a large enough area to map, or areas of abundant small outcrops and bedrock close to the surface but not exposed. The solid color on the maps shows the extent of individual bedrock outcrops; horizontal-line pattern indicates areas of shallow bedrock or areas where small outcrops are too numerous to map individually. In areas of shallow bedrock, the till is typically less than 5 to 10 ft thick.

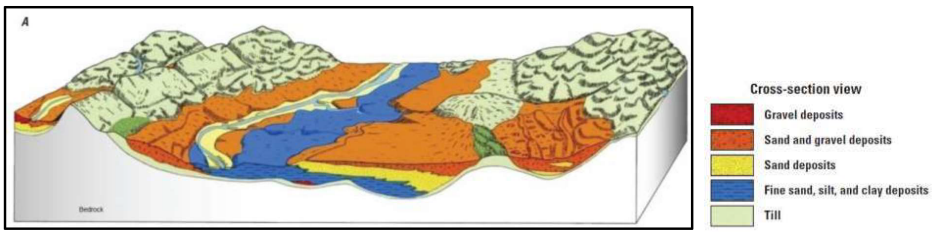

Figure C-1 – Generalized Geologic Section through Surficial Deposits in Central Massachusetts

C.2 - SITE-SPECIFIC SURFICIAL GEOLOGY

The types and extent of surficial geologic materials found beneath the short-listed sites is presented below individually for each site.

C.2.1 - Boston-03

Most of Boston-03 is mapped as coarse glacial stratified deposits, with artificial fill located along the railroad tracks to the west and flood-plain alluvium on either side of Mother Brook that passes through the middle of the site, as shown on Figure C-2.

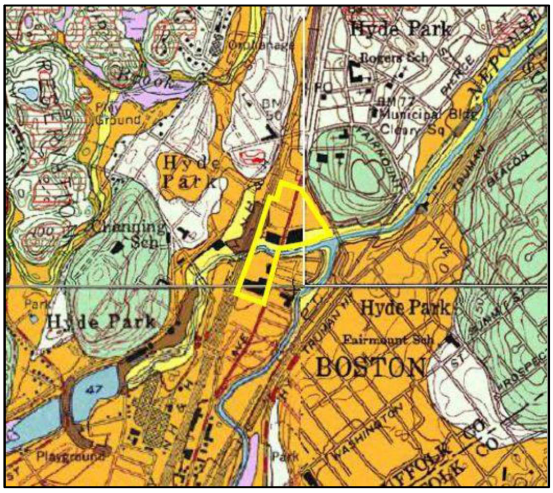

Figure C-2 – Surficial Geologic Deposits – Boston-03 Site

C.2.2 - Worcester-01 and 02

Worcester-01 is underlain entirely by thin till with the north end mapped with shallow bedrock and possible bedrock outcrops, as shown on Figure C-3. The middle of Worcester-02 is underlain by thin till with coarse glacial stratified deposits in the southeast corner and thick till in the northwest corner (extreme southern end of a drumlin).

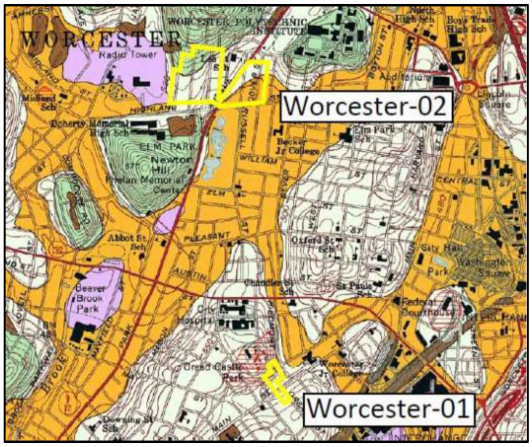

Figure C-3 – Surficial Geologic Deposits – Worcester Sites

C.2.3 - <u>Framingham-01 through 04</u>

Most of the area comprising the Framingham sites is mapped as being underlain by sand and gravel layers deposited by the glaciers that previously occupied the area as they melted. A layer of thin till likely exists throughout the area beneath these deposits and lying on top of the bedrock surface. Much of the area occupied by the Rose Kennedy FHA development and part of the residential area to the south is mapped as thick till, in the form of a drumlin (green oval shading in Figure C-4).

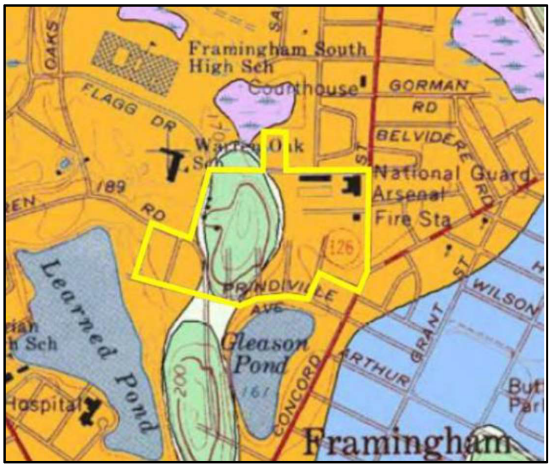

Figure C-4 – Surficial Geologic Deposits – Framingham Sites

C.2.4 - <u>Cambridge-01 and 02</u>

Both Cambridge sites are mapped as glaciomarine fine deposits, as shown on Figure C-5.

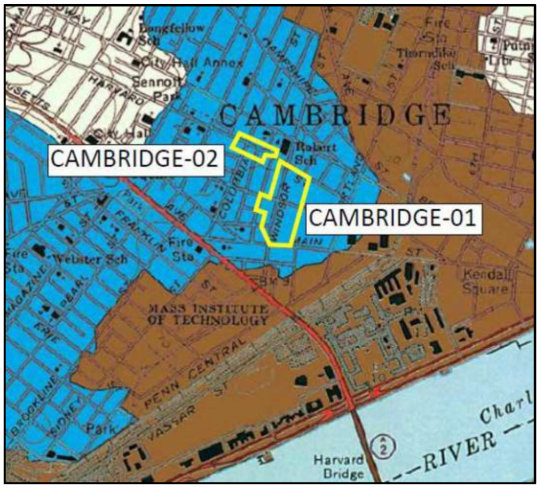

Figure C-5 – Surficial Geologic Deposits – Cambridge Sites

C.3 - BEDROCK GEOLOGY

The major bedrock formations that are mapped to exist beneath the sites that passed Screening 2 are described in Table C-1. All of these formations are metamorphic rocks except for the Cambridge Argillite which is a sedimentary rock. The site locations are shown on Figure C-6 relative to the mapped bedrock formations.

Sites	Bedrock Formation	Geologic Designation	Description
Boston-03	Cambridge Argillite	PzZc	Argillite (mudstone and siltstone), rare sandstone and conglomerate. Contains sandy horizons which are in some places, quartzite.
Worcester-01 and 02	Paxton Formation	Spss	Undifferentiated granofels and schist.
	Worcester Formation	DSw	Carbonaceous slate, phyllite and minor metagraywacke.
Framingham-01 through 04	Unnamed	Zv	Metamorphosed volcanic rock (lava flows and underground magma intrusions)
Cambridge-01 and 02	Cambridge Argillite	PzZc	See above under Boston-03

Table C-1 – Description of Bedrock Formations beneath Screening 2 Sites

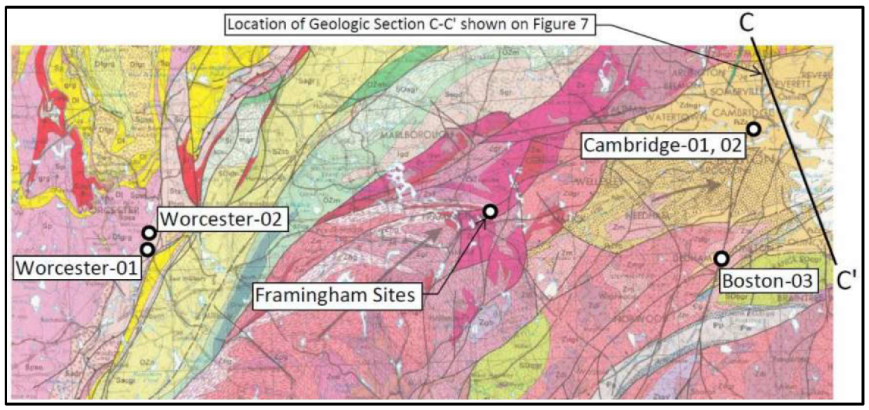

Figure C-6 – USGS Regional Bedrock Mapping within the Area of the Sites

The mapping shown on Figure C-**6 represents the "first" rock that would be encountered** when drilling a geothermal loop from the surface downwards. Going deeper it is possible that drilling will encounter other bedrock formations because the rock is typically deformed and inclined as a result of past tectonic activity (earth plate movement). Figure C-7 is a portion of a geologic section through Boston illustrating how the orientation and distribution of bedrock formations varies with depth (note the vertical scale in this figure is greatly exagerrated for visualization purposes).

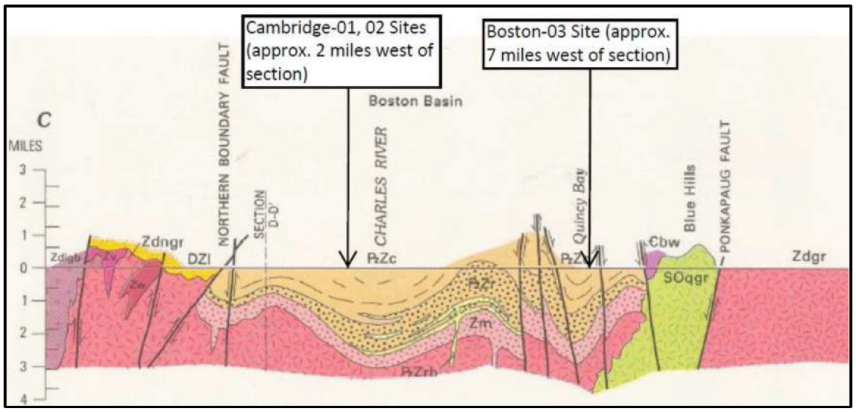

Figure C-7 – Example Geologic Section through Bedrock Formations near Boston and Cambridge Sites (see Line of Section C-C' on Figure 6)

C.4 – REGIONAL THERMAL CONDUCTIVITY

Thermal conductivity (TC) is a measure of how easily heat moves through the earth and is a primary determining factor for the size of the geothermal borefield **needed to meet a district system's heating** and cooling demand. A high TC optimizes the heat exchange between the borefield and the ground, thus minimizes the size and construction cost of the borefield. Estimated TC for the geologic materials beneath the potential pilot sites was used in the KT ranking described in the Final Site Recommendation Report.

Research into online sources of TC data from near the potential pilot sites was performed. One source is illustrated in Figure C-8 presenting bedrock TC measurements collected throughout Massachusetts in 2013 as part of the Massachusetts Geothermal Energy Project (MGEP). As shown on the figure, no specific data are available for locations in proximity to any of the potential pilot sites. However, measured TC values from the MGEP study were correlated to general bedrock type, or lithology, some of which are present beneath the pilot sites. Table 2 shows these correlations. For example, the Boston-03 site is underlain by argillite, which is a sedimentary rock that correlates from the MGEP to a TC of less than 1.15 Btu/hr-ft-°F.

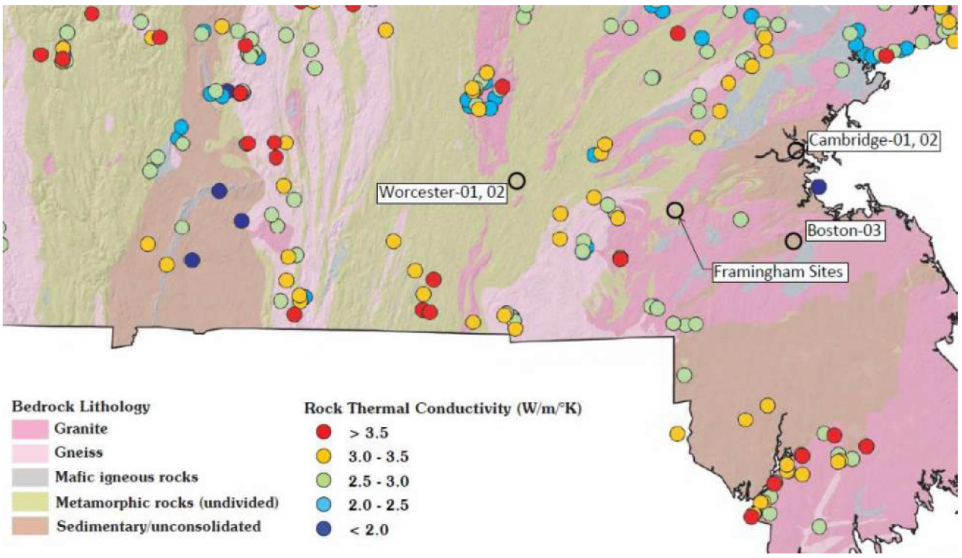

Figure C-8 – Bedrock Thermal Conductivity Measurements in Massachusetts, 2013

Sites	Bedrock Formation Name	Bedrock Type	Bedrock Lithology	Thermal Conductivity (Btu/hr-ft-°F)	
			From MGEP, Figure C-8 *		Other Sources **
Boston-03	Cambridge Argillite	Argillite	Sedimentary rocks	<1.15	1.56, 1.68, 1.74, 1.92, 2.03
Worcester-01 and 02	Paxton Formation	Mica schist	Metamorphic rocks	1.15-1.44	1.67

	Worcester Formation	Slate, Phyllite	Metamorphic rocks	1.15-1.44	1.67
Framingham Sites	Unnamed	Metamorphosed volcanics	Metamorphic rocks	1.15-1.44	1.78, 1.89, 2.03
Cambridge-01 and 02	Cambridge Argillite	Argillite	Sedimentary rocks	<1.15	1.56, 1.68, 1.74, 1.92, 2.03

* From Massachusetts Geothermal Energy Project, 2013, see Figure C-8. Values converted to Btu/hr-ft-°F.

** From internal records of CDM Smith, Inc. and Tracey A. Ogden Geothermal & Drilling Consultant. Sources cannot be disclosed due to client privacy. Measurements from standard borehole thermal response tests, test loop depths range from 500 ft to 1,500 ft.

Table C-2 – Thermal Conductivity Data

Inspection of the TC values from the MGEP showed them to be significantly lower than typical industry values obtained from actual thermal response tests performed on geothermal test loops. The CDM Smith team gathered results for test loops installed near the potential pilot sites and compared the data to the MGEP data. These data are presented in the far right column in Table C-2 under Other Sources. These data are considered to be more accurate than the MGEP data, which are from tests run on small samples of various bedrock types collected from surface outcrops and not from actual test loops.

C.5 – FRAMINGHAM SITES DETAILED GEOLOGY

C.5.1 – Surficial Geology

Figure C-9 is a geologic section illustrating the relationship between the various glacial surficial deposits that occur in central and eastern Massachusetts, including the area of the Framingham sites. Note the hilly nature of the thick till in the form of drumlins (QT), which were formed beneath the glaciers, and the glacial stratified materials (Qlcn, Qlcb, and Qal) that were deposited later between and along the flanks of the drumlins as the glaciers melted.

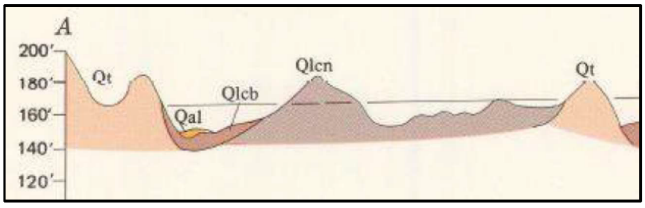

Figure C-9 – Geologic Section through Thick Till (Drumlins, "Qt") and Glacial Stratified Deposits in Framingham

C.5.2 – Bedrock Geology

There are four bedrock formations mapped to exist beneath the Framingham sites that are very old (mostly Precambrian age) as shown on Figure C-10 (plan view) and described below.

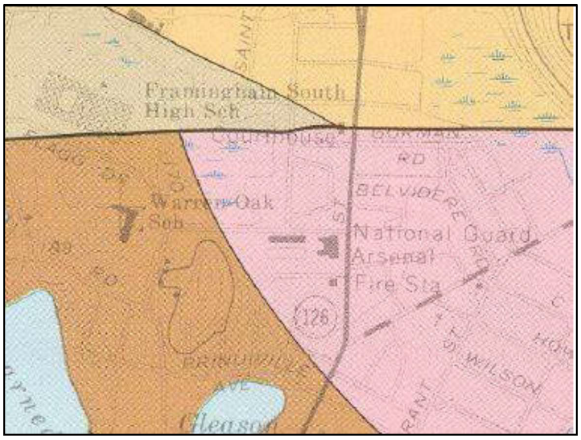

Figure C-10 – Mapped Bedrock Formations beneath Framingham Sites

PzpCmr

Mixed Rocks (PzpCmr) is a grouping of Precambrian age, interlayered rock types that vary in composition and include metamorphosed volcanic rocks, conglomerate, quartzite, slate, and schist. The rock textures range from very fine- to medium-grained. A large variation in minerals occurs across the different rock types. It is reported to be as much as 2,000 meters thick.

dg

Dedham Granodiorite (dg) is a Precambrian age, fine- to coarse-grained metamorphic rock that is mostly granodiorite. The principal minerals are quartz, perthite and microcline, plagioclase, biotite, and muscovite. The rock texture varies widely, **ranging from "massive" (solid crystalline rock, no fractures or faults) to containing** intrusions, faults or other openings that have been filled in with other rock types over its geologic history. Locally it is severely deformed.

m

Milford Granite (m) is a Proterozoic Z-age, fine- to coarse-grained metamorphic rock like the Dedham Granodiorite except it ranges from granite to granodiorite. The principal minerals are quartz, perthite and microcline, albite, biotite, and muscovite. In places there are large mineral crystals embedded in the rock matrix.

pCw

Westboro Quartzite (pCw) is a Precambrian age, mostly fine-grained quartzite. Its texture varies from massive to interlayered with other rock types including schist and gneiss. It is reported to be as much as 1,200 meters thick.

Figure C-11 is a north-south oriented geologic section east of the Framingham sites showing the occurrence of three of the formations (Mixed Rocks, Dedham Granodiorite, and Milford Granite). Based on this published information, the bedrock beneath the project site is inferred to be hard and could be moderately to extensively fractured and faulted.

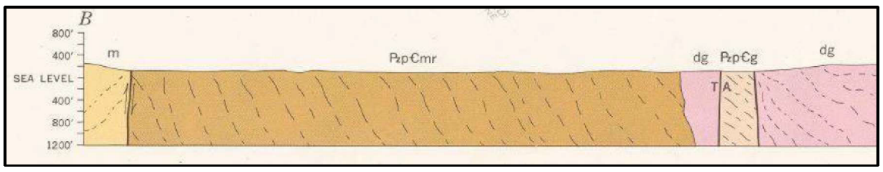

Figure C-11 – Geologic Section East of the Framingham Sites Showing the Mixed Rocks, Dedham Granodiorite, and Milford Granite Bedrock Formations

C.5.3 – <u>Depth to Bedrock</u>

Figure C-12 shows the recorded depth to bedrock near the Framingham sites obtained from the MassDEP well records database, and from a geothermal test hole drilled at Mass Bay Community College, as noted. The depth to bedrock beneath the sand and gravel deposits around the Framingham sites is estimated to range from 14 feet to 70 feet below land surface based on the available data. The proposed borefields north of Normandy Road and along Concord Street near the firehouse are located over these deposits, therefore, depth to rock during drilling geothermal loops at these borefields can be expected to fall within this range.

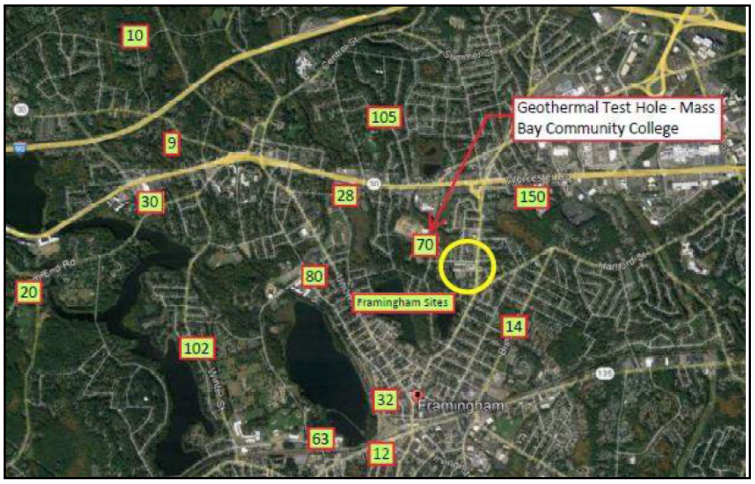

Figure C-12 – Depth to Bedrock near Framingham Sites from MassDEP Well Records and Geothermal Test Hole Drilled at Mass Bay Community College

Surface elevations at the borefield in the Rose Kennedy public housing development (beneath the drumlin) are on the order of 40 feet higher than surrounding areas. Depth to rock may be as much as 40 feet deeper here than the other borefields unless the drumlin has a bedrock knob core, in which case depth to rock may be comparable to the other borefield areas. It should be noted that bedrock depth can vary significantly across an area, even within relatively short distances between locations, and actual bedrock depth can best be determined through test drilling.

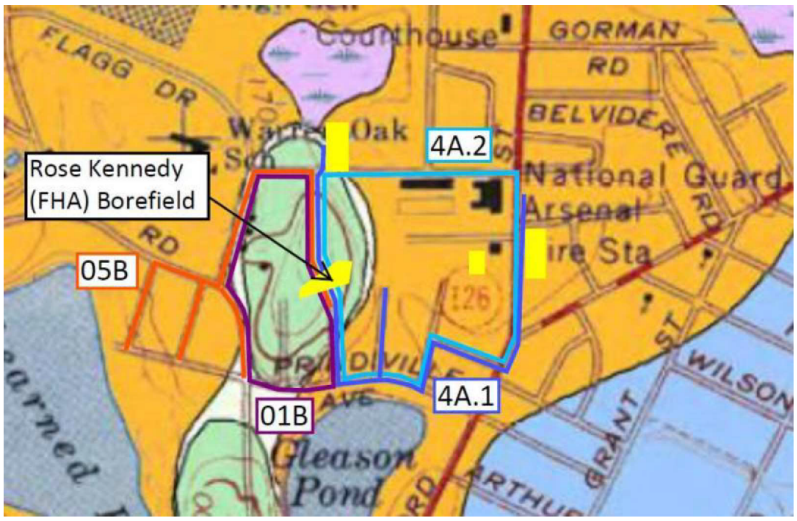

Figure C-10 – Locations of Framingham Sites Relative to Surficial Geologic Deposits

C.6 - LIMITATIONS

The following should be noted relative to the above description of the geologic materials that occur at the sites:

- For all the sites, where thin till does not exist at the surface, it likely exists overlying the bedrock surface and beneath the other mapped geologic materials.
- The above discussion is based on subsurface conditions inferred from publicly available, published geologic documents. The subsurface conditions mentioned herein are only approximate and are inferred and may vary from actual conditions encountered at the site.
- This review of available information provides insight into what conditions may exist and be anticipated. No level of due diligence can replace the actual drilling of wells. Actual subsurface conditions should be documented in the field under the supervision of a qualified professional geologist or geotechnical engineer during drilling.

APPENDIX B: THERMAL RESPONSE TEST PROCEDURE AND ANALYSIS

TEST PROCEDURES

The American Society of Heating, Refrigeration, and Air-Conditioning Engineers (ASHRAE) has published recommended procedures for performing formation thermal conductivity tests in the ASHRAE HVAC Applications Handbook, Geothermal Energy Chapter. The International Ground Source Heat Pump Association (IGSHPA) also lists test procedures in their Design and Installation Standards. GRTI's test procedures meet or exceed those recommended by ASHRAE and IGSHPA, with the specific procedures described below:

Grouting Procedure for Test Loops – To ensure against bridging and voids, it is recommended that the bore annulus is uniformly grouted from the bottom to the top via tremie pipe.

Time Between Loop Installation and Testing – A minimum delay of five days between loop installation and test startup is recommended for bores that are air drilled, and a minimum waiting period of two days for mud rotary drilling.

Undisturbed Formation Temperature Measurement – The undisturbed formation temperature should be determined by recording the loop temperature as the water returns from the u-bend at test startup.

Required Test Duration – A minimum test duration of 36 hours is recommended, with a preference toward 48 hours.

Data Acquisition Frequency - Test data is recorded at five minute intervals.

Equipment Calibration/Accuracy – Transducers and datalogger are calibrated per manufacturer recommendations. Manufacturer stated accuracy of power transducers is less than ±2%. Temperature sensor accuracy is periodically checked via ice water bath.

Power Quality – The standard deviation of the power should be less than or equal to 1.5% of the average power, with maximum power variation of less than or equal to 10% of the average power.

Input Heat Rate – The heat flux rate should be 51 Btu/hr (15 W) to 85 Btu/hr (25 W) per foot of installed bore depth to best simulate the expected peak loads on the u-bend.

Insulation – GRTI's equipment has 1 inch of foam insulation on the FTC unit and 1/2 inch of insulation on the hose kit connection. An additional 2 inches of insulation is provided for both the FTC unit and loop connections by insulating blankets.

Retesting in the Event of Failure – In the event that a test fails prematurely, a retest may not be performed until the bore temperature is within 0.5°F of the original undisturbed formation temperature or until a period of 14 days has elapsed.

Figure B–1 Procedure used for thermal response test (reference: GRTI thermal response test report and analysis)

DATA ANALYSIS

Geothermal Resource Technologies, Inc. (GRTI) uses the "line source" method of data analysis to determine the thermal conductivity of the formation. The line source method assumes an infinitely thin line source of heat in a continuous medium. A plot of the late-time temperature rise of the line source temperature versus the natural log of elapsed time will follow a linear trend. The linear slope is inversely proportional to the thermal conductivity of the medium. Applying the line source method to a u-bend grouted in a borehole, the test must be run long enough to allow the finite dimensions of the u-bend pipes and the grout to become insignificant. Experience has shown that approximately ten hours is required to allow the error of early test times and the effects of finite borehole dimensions to become insignificant.

In order to analyze real data from a formation thermal conductivity test, the average temperature of the water entering and exiting the u-bend heat exchanger is plotted versus the natural log of elapsed testing time. Using the Method of Least Squares, linear coefficients are then calculated to produce a line that fits the data. This procedure is repeated for various time intervals to ensure that variations in the power or other effects are not producing inaccurate results.

Bore thermal resistance was determined using the formula outlined in Gehlin's Doctoral Thesis[2]. A serial development was used to approximate the exponential integral. The calculated bore resistance applies only to the test conditions, a bore in an operating loopfield could have a significantly different resistance due to changes in the loop fluid temperature, flow rate and presence of antifreeze.

The calculated results are based on test bore information submitted by the driller/testing agency. GRTI is not responsible for inaccuracies in the results due to erroneous bore information. All data analysis is performed by personnel that have an engineering degree from an accredited university with a background in heat transfer and experience with line source theory. The test results apply specifically to the tested bore. Additional bores at the site may have significantly different results depending upon variations in geology and hydrology.

Through the analysis process, the collected raw data is converted to spreadsheet format (Microsoft Excel®) for final analysis. If desired, please contact GRTI and a copy of the data will be made available in either a hard copy or electronic format.

CONTACT: Chad Martin
Regional Managing Engineer
Asheville, NC
(828) 225-9166
cmartin@grti.com

Figure B–2 Data Analysis used in the GRTI thermal response test report and analysis.

APPENDIX C: FARLEY PARKING LOT GEOTHERMAL BOREHOLE GRTI TRT REPORT

Below are the snippets from the GRTI report on the Farley Parking Lot geothermal borehole.

FORMATION THERMAL CONDUCTIVITY
TEST & DATA ANALYSIS

TEST LOCATION	**Eversource, Test Bore 2** **Farley Lot** **Framingham, MA**
TEST DATE	October 13-15, 2022
ANALYSIS FOR	Skillings & Sons, Inc. 9 Columbia Drive Amherst, NH 03031 Phone: (603) 459-2600
TEST PERFORMED BY	Skillings & Sons, Inc.

WESTERN OFFICE
PO Box 256, Elkton, SD 57026
P: 866-991-4784 F: 605-542-5391

EASTERN OFFICE
6 William Warren Dr, Asheville, NC 28806
P: 828-275-7113

EXECUTIVE SUMMARY

A formation thermal conductivity test was performed on geothermal Test Bore 2 at the Farley Lot site in Framingham, Massachusetts. The vertical bore was installed on September 22-23, 2022 by Skillings & Sons, Inc. Geothermal Resource Technologies' (GRTI) test unit was attached to the vertical bore on the afternoon of October 13, 2022.

This report provides an overview of the test procedures and analysis process, along with plots of the loop temperature and input heat rate data. The collected data was analyzed using the "line source" method and the following average formation thermal conductivity was determined.

Formation Thermal Conductivity = 1.78 Btu/hr-ft-°F

Due to the necessity of a thermal diffusivity value in the design calculation process, an estimate of the average thermal diffusivity was made for the encountered formation.

Formation Thermal Diffusivity ≈ 1.10 ft^2/day

Bore thermal resistance calculations were made on the test data using the method outlined in the Gehlin Doctoral Thesis[1]. Since the average value listed below was empirically determined from the test data it may not directly correlate with values found in loopfield design programs.

Bore Thermal Resistance = 0.245 hr-ft-°F/Btu

The undisturbed formation temperature for the tested bore was established from the initial loop temperature data collected at startup.

Undisturbed Formation Temperature ≈ 53.3-54.1°F

The formation thermal properties determined by this test do not directly translate into a loop length requirement (i.e. feet of bore per ton). These parameters, along with many others, are inputs to commercially available loop-field design software to determine the required loop length. Additional questions concerning the use of these results are discussed in the frequently asked question (FAQ) section at www.grti.com.

[1] Signhild Gehlin. "Thermal Response Test - Method Development and Evaluation," (Doctoral Thesis, Lulea University of Technology, 2002).

Test Bore Details

(As Provided by Skillings & Sons, Inc.)

Site Name	Eversource, Farley Lot, Test Bore 2
Location	Framingham, MA
Driller	Skillings & Sons, Inc.
Installed Date	September 22-23, 2022
Borehole Diameter	6 inches
Casing	Permanent 6 inch steel casing from 0-80 ft
U-Bend Size	1-1/4 inch HDPE
U-Bend Depth Below Grade	615 ft
Grout Type	GeoPro TG Lite/PowerTEC 1.4
Grout Mixture	150 lb TG Select, 64 lb PowerTEC, 48 gallons water

Drill Log

Formation Description	Depth (ft)
Overburden (brown and gray boulders and silty clay)	0'-60'
Light grey, grey, and pink diorite	60'-615'

Note: Boulders from 53-60 ft made casing installation difficult. Bore also produced 2 gpm water from 460-480ft.

THERMAL CONDUCTIVITY TEST DATA

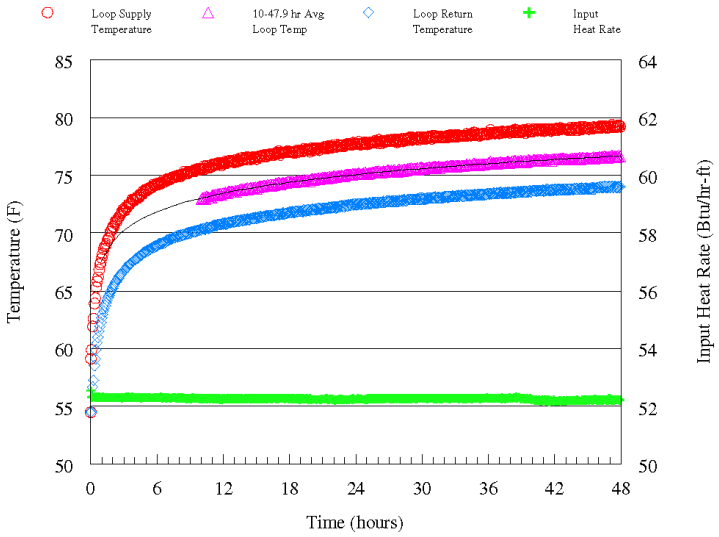

FIG. 1: TEMPERATURE & HEAT RATE DATA VS TIME

Figure 1 above shows the loop temperature and heat input rate data versus the elapsed time of the test. The temperature of the fluid supplied to and returning from the U-bend are plotted on the left axis, while the amount of heat supplied to the fluid is plotted on the right axis on a per foot of bore basis. In the test statistics below, calculations on the power data were performed over the analysis time period listed in the Line Source Data Analysis section.

SUMMARY TEST STATISTICS

Test Date	October 13-15, 2022
Undisturbed Formation Temperature	Approx. 53.3-54.1°F
Duration	47.9 hr
Average Voltage	238.7 V
Average Heat Input Rate	32,138 Btu/hr (9,416 W)
Avg Heat Input Rate per Foot of Bore	52.3 Btu/hr-ft (15.3 W/ft)
Circulator Flow Rate	12.3 gpm
Standard Deviation of Power	0.05%
Maximum Variation in Power	0.19%

LINE SOURCE DATA ANALYSIS

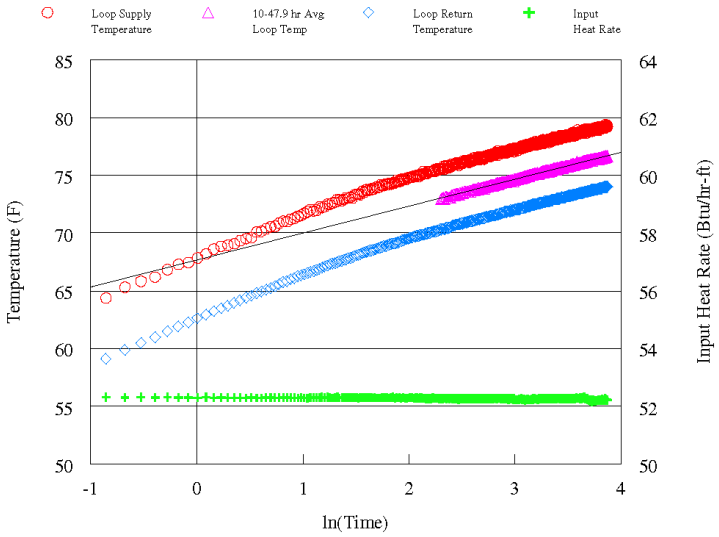

FIG. 2: TEMPERATURE & HEAT RATE VS NATURAL LOG OF TIME

The loop temperature and input heat rate data versus the natural log of elapsed time are shown above in Figure 2. The temperature versus time data was analyzed using the line source method (see page 3) in conformity with ASHRAE and IGSHPA guidelines. A linear curve fit was applied to the average of the supply and return loop temperature data between 10 and 47.9 hours. The slope of the curve fit was found to be 2.33. The resulting thermal conductivity was found to be **1.78 Btu/hr-ft-°F**.

THERMAL DIFFUSIVITY

The reported drilling log for this test borehole indicated that the formation consisted of overburden consisting of silty clay and boulders and diorite bedrock. An average heat capacity value for diorite was calculated from specific heat and density values listed by Kavanaugh and Rafferty[3]. A weighted average of heat capacity values based on the indicated formation was used to determine an average heat capacity of 39.1 Btu/ft^3-°F for the formation. A diffusivity value was then found using the calculated formation thermal conductivity and the estimated heat capacity. The thermal diffusivity for this formation was estimated to be **1.10 ft^2/day**.

[3] Stephen P. Kavanaugh and Kevin Rafferty, Geothermal Heating and Cooling: Design of Ground-Source Heat Pump Systems (Atlanta: ASHRAE, 2014), 75.

BORE THERMAL RESISTANCE

Resistance to heat transfer from a geothermal bore can be viewed as consisting of two components, bore resistance and ground resistance. This relationship is diagrammed in Figure 3, where t_f is the loop fluid temperature, t_b is the bore wall temperature and t_g is the ground temperature. The ground resistance is dependent upon the formation thermal conductivity and diffusivity. Factors that affect bore thermal resistance include the resistance of the pipe material, diameter of the heat exchanger, position of the heat exchanger in the bore, the bore diameter, casing length and type, and the thermal conductivity of the grout/backfill in the bore annulus. A detailed examination of bore resistance is discussed by Kavanaugh and Rafferty[4].

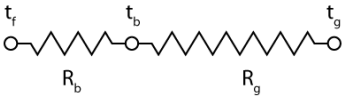

FIG. 3: RESISTANCE DIAGRAM FOR A GEOTHERMAL BORE

Bore thermal resistance calculations were made on the test data according to the formula below as outlined in the Gehlin Doctoral Thesis[5]. The calculated formation thermal conductivity and thermal diffusivity from the Line Source Analysis were used in the formula. The average undisturbed formation temperature of 53.7°F was used and the average bore thermal resistance from 10-47.9 hrs was found to be **0.245 hr-ft-°F/Btu**.

The calculated bore resistances apply only to the test conditions, and a bore in an operating loopfield could have a significantly different resistance due to changes in the loop fluid temperature, flow rate, and presence of antifreeze. Additional information on bore resistance may be found in the study by Oklahoma State University and Oklahoma Gas & Electric where various vertical bore heat exchanger configurations were tested[6].

$$R_b = \frac{H}{Q} * \left\{ T(t) - T_g - \frac{Q}{4\pi\lambda_g H} * \left[Ei\left(\frac{r_b^2}{4\alpha_g t} \right) \right] \right\}$$

Where:

	R_b	Borehole thermal resistance (hr-ft-°F/Btu)
	H	Active U-bend depth (ft)
	Q	Average heat injected (Btu/hr)
	$T(t)$	Temperature dependent on time t (°F)
	T_g	Undisturbed ground temperature
	λ_g	Formation thermal conductivity (Btu/hr-ft-°F)
	r_b	Average borehole radius (in)
	α_g	Formation thermal diffusivity (ft^2/hr)

[4]Stephen P. Kavanaugh and Kevin Rafferty, Geothermal Heating and Cooling: Design of Ground-Source Heat Pump Systems (Atlanta: ASHRAE, 2014), pages 58-67.
[5]Gehlin, 12-13.
[6] Beier, R. and Ewbank, G. (2012, August). *In-Situ Test Thermal Response Tests Interpretations, OG&E Ground Source Heat Exchange Study*. Retrieved from http://ghpok.org/

APPENDIX D: ROSE KENNEDY GEOTHERMAL BOREHOLE GRTI TRT REPORT

Below are the snippets from the GRTI report on the Rose Kennedy geothermal borehole.

GRTI

FORMATION THERMAL CONDUCTIVITY
TEST & DATA ANALYSIS

TEST LOCATION **Eversource, Test Bore 3**
Rose Kennedy Lane
Framingham, MA

TEST DATE October 19-21, 2022

ANALYSIS FOR Skillings & Sons, Inc.
9 Columbia Drive
Amherst, NH 03031
Phone: (603) 459-2600

TEST PERFORMED BY Skillings & Sons, Inc.

WESTERN OFFICE
PO Box 256, Elkton, SD 57026
P: 866-991-4784 F: 605-542-5391

EASTERN OFFICE
6 William Warren Dr, Asheville, NC 28806
P: 828-275-7113

EXECUTIVE SUMMARY

A formation thermal conductivity test was performed on geothermal Test Bore 3 at the Rose Kennedy Lane site in Framingham, Massachusetts. The vertical bore was installed on September 28, 2022 by Skillings & Sons, Inc. Geothermal Resource Technologies' (GRTI) test unit was attached to the vertical bore on the afternoon of October 19, 2022.

This report provides an overview of the test procedures and analysis process, along with plots of the loop temperature and input heat rate data. The collected data was analyzed using the "line source" method and the following average formation thermal conductivity was determined.

Formation Thermal Conductivity = 1.57 Btu/hr-ft-°F

Due to the necessity of a thermal diffusivity value in the design calculation process, an estimate of the average thermal diffusivity was made for the encountered formation.

Formation Thermal Diffusivity ≈ 0.98 ft^2/day

Bore thermal resistance calculations were made on the test data using the method outlined in the Gehlin Doctoral Thesis[1]. Since the average value listed below was empirically determined from the test data it may not directly correlate with values found in loopfield design programs.

Bore Thermal Resistance = 0.251 hr-ft-°F/Btu

The undisturbed formation temperature for the tested bore was established from the initial loop temperature data collected at startup.

Undisturbed Formation Temperature ≈ 53.2-54.3°F

The formation thermal properties determined by this test do not directly translate into a loop length requirement (i.e. feet of bore per ton). These parameters, along with many others, are inputs to commercially available loop-field design software to determine the required loop length. Additional questions concerning the use of these results are discussed in the frequently asked question (FAQ) section at www.grti.com.

[1] Signhild Gehlin. "Thermal Response Test - Method Development and Evaluation," (Doctoral Thesis, Lulea University of Technology, 2002).

TEST BORE DETAILS
(AS PROVIDED BY SKILLINGS & SONS, INC.)

Site Name	Eversource, Rose Kennedy Lane
Location	Framingham, MA
Driller	Skillings & Sons, Inc.
Installed Date	September 28, 2022
Borehole Diameter	6 inches
Casing	Permanent 6 inch steel casing from 0-150 ft
U-Bend Size	1-1/4 inch HDPE
U-Bend Depth Below Grade	610 ft
Grout Type	GeoPro TG Lite/PowerTEC 1.4
Grout Mixture	150 lb TG Select, 64 lb PowerTEC, 48 gallons water

DRILL LOG

FORMATION DESCRIPTION	DEPTH (FT)
Overburden (brown cobbles, boulders, and clay)	0'-136'
Grey Diorite	136'-610'

Note: Bore produced 2 gpm water at 460-480 ft.

THERMAL CONDUCTIVITY TEST DATA

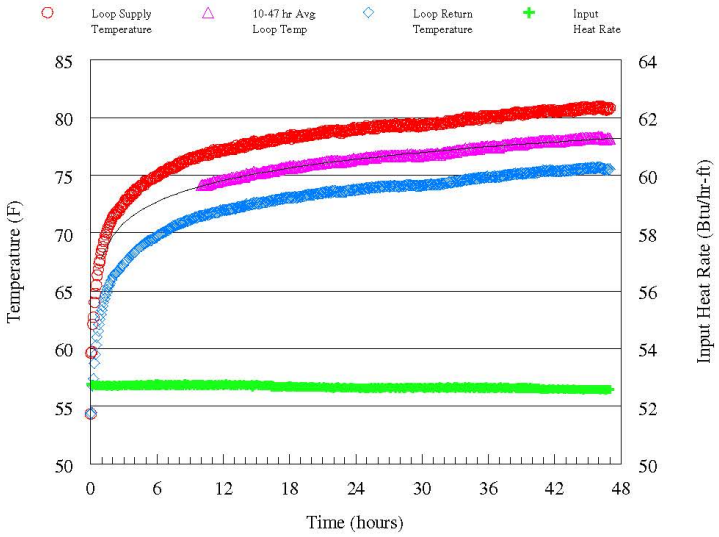

FIG. 1: TEMPERATURE & HEAT RATE DATA VS TIME

Figure 1 above shows the loop temperature and heat input rate data versus the elapsed time of the test. The temperature of the fluid supplied to and returning from the U-bend are plotted on the left axis, while the amount of heat supplied to the fluid is plotted on the right axis on a per foot of bore basis. In the test statistics below, calculations on the power data were performed over the analysis time period listed in the Line Source Data Analysis section.

SUMMARY TEST STATISTICS

Test Date	October 19-21, 2022
Undisturbed Formation Temperature	Approx. 53.2-54.3°F
Duration	47.0 hr
Average Voltage	238.8 V
Average Heat Input Rate	32,119 Btu/hr (9,411 W)
Avg Heat Input Rate per Foot of Bore	52.7 Btu/hr-ft (15.4 W/ft)
Circulator Flow Rate	12.3 gpm
Standard Deviation of Power	0.09%
Maximum Variation in Power	0.23%

LINE SOURCE DATA ANALYSIS

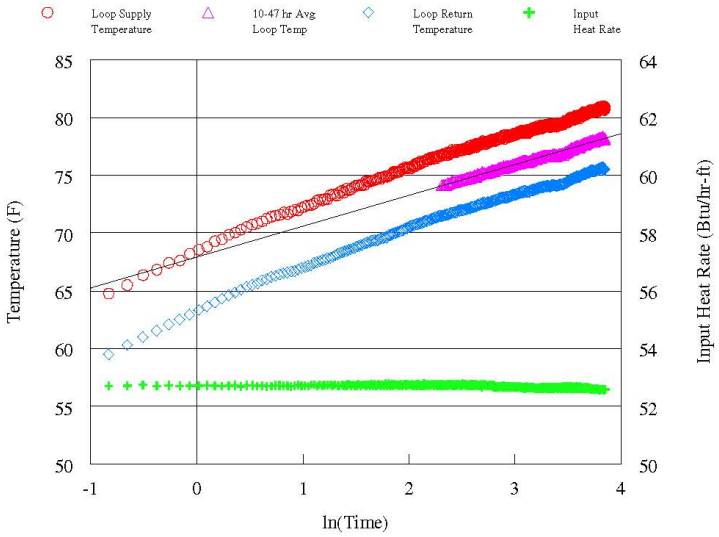

FIG. 2: TEMPERATURE & HEAT RATE VS NATURAL LOG OF TIME

The loop temperature and input heat rate data versus the natural log of elapsed time are shown above in Figure 2. The temperature versus time data was analyzed using the line source method (see page 3) in conformity with ASHRAE and IGSHPA guidelines. A linear curve fit was applied to the average of the supply and return loop temperature data between 10 and 47.0 hours. The slope of the curve fit was found to be 2.66. The resulting thermal conductivity was found to be **1.57 Btu/hr-ft-°F**.

THERMAL DIFFUSIVITY

The reported drilling log for this test borehole indicated that the formation consisted of clay, cobbles, boulders and diorite bedrock. A heat capacity values for diorite was calculated from specific heat and density values listed by Kavanaugh and Rafferty[3]. A weighted average of heat capacity values based on the indicated formation was used to determine an average heat capacity of 38.4 Btu/ft^3-°F for the formation. A diffusivity value was then found using the calculated formation thermal conductivity and the estimated heat capacity. The thermal diffusivity for this formation was estimated to be **0.98 ft^2/day**.

[3] Stephen P. Kavanaugh and Kevin Rafferty, Geothermal Heating and Cooling: Design of Ground-Source Heat Pump Systems (Atlanta: ASHRAE, 2014), 75.

BORE THERMAL RESISTANCE

Resistance to heat transfer from a geothermal bore can be viewed as consisting of two components, bore resistance and ground resistance. This relationship is diagrammed in Figure 3, where t_f is the loop fluid temperature, t_b is the bore wall temperature and t_g is the ground temperature. The ground resistance is dependent upon the formation thermal conductivity and diffusivity. Factors that affect bore thermal resistance include the resistance of the pipe material, diameter of the heat exchanger, position of the heat exchanger in the bore, the bore diameter, casing length and type, and the thermal conductivity of the grout/backfill in the bore annulus. A detailed examination of bore resistance is discussed by Kavanaugh and Rafferty[4].

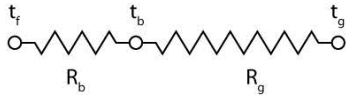

FIG. 3: RESISTANCE DIAGRAM FOR A GEOTHERMAL BORE

Bore thermal resistance calculations were made on the test data according to the formula below as outlined in the Gehlin Doctoral Thesis[5]. The calculated formation thermal conductivity and thermal diffusivity from the Line Source Analysis were used in the formula. The average undisturbed formation temperature of 53.8°F was used and the average bore thermal resistance from 10-47.0 hrs was found to be **0.251 hr-ft-°F/Btu** .

The calculated bore resistances apply only to the test conditions, and a bore in an operating loopfield could have a significantly different resistance due to changes in the loop fluid temperature, flow rate, and presence of antifreeze. Additional information on bore resistance may be found in the study by Oklahoma State University and Oklahoma Gas & Electric where various vertical bore heat exchanger configurations were tested[6].

$$R_b = \frac{H}{Q} * \left\{ T(t) - T_g - \frac{Q}{4\pi\lambda_g H} * \left[Ei\left(\frac{r_b^2}{4\alpha_g t}\right)\right]\right\}$$

Where:

	R_b	Borehole thermal resistance (hr-ft-°F/Btu)
	H	Active U-bend depth (ft)
	Q	Average heat injected (Btu/hr)
	$T(t)$	Temperature dependent on time t (°F)
	T_g	Undisturbed ground temperature
	λ_g	Formation thermal conductivity (Btu/hr-ft-°F)
	r_b	Average borehole radius (in)
	α_g	Formation thermal diffusivity (ft^2/hr)

[4]Stephen P. Kavanaugh and Kevin Rafferty, Geothermal Heating and Cooling: Design of Ground-Source Heat Pump Systems (Atlanta: ASHRAE, 2014), pages 58-67.
[5]Gehlin, 12-13.
[6] Beier, R. and Ewbank, G. (2012, August). *In-Situ Test Thermal Response Tests Interpretations, OG&E Ground Source Heat Exchange Study*. Retrieved from http://ghpok.org/

APPENDIX E: FIRE STATION GEOTHERMAL BOREHOLE GRTI TRT REPORT

Below are the snippets from the GRTI report on the Fire Station geothermal borehole.

FORMATION THERMAL CONDUCTIVITY
TEST & DATA ANALYSIS

TEST LOCATION **Eversource, Test Bore 1**
Fire Department
Framingham, MA

TEST DATE October 17-19, 2022

ANALYSIS FOR Skillings & Sons, Inc.
9 Columbia Drive
Amherst, NH 03031
Phone: (603) 459-2600

TEST PERFORMED BY Skillings & Sons, Inc.

WESTERN OFFICE
PO Box 256, Elkton, SD 57026
P: 866-991-4784 F: 605-542-5391

EASTERN OFFICE
6 William Warren Dr, Asheville, NC 28806
P: 828-275-7113

EXECUTIVE SUMMARY

A formation thermal conductivity test was performed on geothermal Test Bore 1 at the Fire Department site in Framingham, Massachusetts. The vertical bore was installed on September 22, 2022 by Skillings & Sons, Inc. Geothermal Resource Technologies' (GRTI) test unit was attached to the vertical bore on the morning of October 17, 2022.

This report provides an overview of the test procedures and analysis process, along with plots of the loop temperature and input heat rate data. The collected data was analyzed using the "line source" method and the following average formation thermal conductivity was determined.

Formation Thermal Conductivity = 1.92 Btu/hr-ft-°F

Due to the necessity of a thermal diffusivity value in the design calculation process, an estimate of the average thermal diffusivity was made for the encountered formation.

Formation Thermal Diffusivity ≈ 1.28 ft^2/day

Bore thermal resistance calculations were made on the test data using the method outlined in the Gehlin Doctoral Thesis[1]. Since the average value listed below was empirically determined from the test data it may not directly correlate with values found in loopfield design programs.

Bore Thermal Resistance = 0.236 hr-ft-°F/Btu

The undisturbed formation temperature for the tested bore was established from the initial loop temperature data collected at startup.

Undisturbed Formation Temperature ≈ 53.5-54.1°F

The formation thermal properties determined by this test do not directly translate into a loop length requirement (i.e. feet of bore per ton). These parameters, along with many others, are inputs to commercially available loop-field design software to determine the required loop length. Additional questions concerning the use of these results are discussed in the frequently asked question (FAQ) section at www.grti.com.

[1] Signhild Gehlin. "Thermal Response Test - Method Development and Evaluation," (Doctoral Thesis, Lulea University of Technology, 2002).

Test Bore Details

(As Provided by Skillings & Sons, Inc.)

Site Name	Eversource, Fire Station, Test Bore 1
Location	Framingham, MA
Driller	Skillings & Sons, Inc.
Installed Date	September 22, 2022
Borehole Diameter	6 inches
Casing	Permanent 6 inch steel casing from 0-110 ft
U-Bend Size	1-1/4 inch HDPE
U-Bend Depth Below Grade	610 ft
Grout Type	GeoPro TG Lite/PowerTEC 1.4
Grout Mixture	150 lb TG Select, 64 lb PowerTEC, 48 gallons water

Drill Log

Formation Description	Depth (ft)
Overburden (brown cobbles, fine sand)	0'-84'
Grey Diorite, Gabbro	84'-610'

Note: Bore produced 8 gpm water at 233-236 ft.

THERMAL CONDUCTIVITY TEST DATA

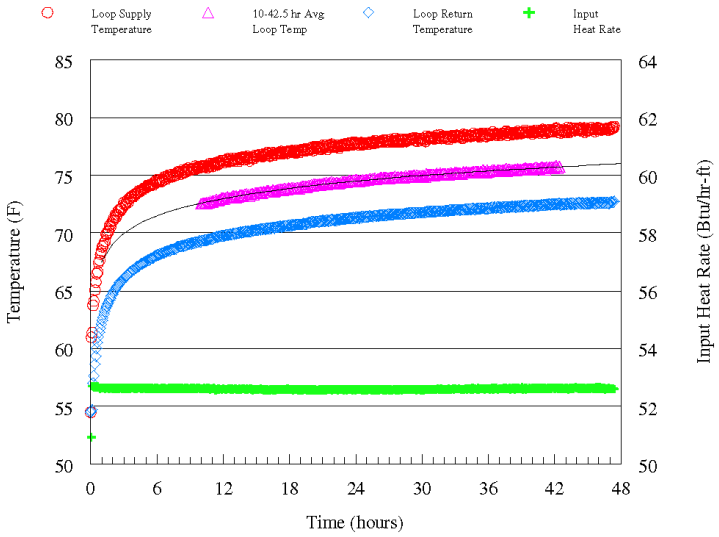

FIG. 1: TEMPERATURE & HEAT RATE DATA VS TIME

Figure 1 above shows the loop temperature and heat input rate data versus the elapsed time of the test. The temperature of the fluid supplied to and returning from the U-bend are plotted on the left axis, while the amount of heat supplied to the fluid is plotted on the right axis on a per foot of bore basis. In the test statistics below, calculations on the power data were performed over the analysis time period listed in the Line Source Data Analysis section.

SUMMARY TEST STATISTICS

Test Date	October 17-19, 2022
Undisturbed Formation Temperature	Approx. 53.5-54.1°F
Duration	47.4 hr
Average Voltage	238.8 V
Average Heat Input Rate	32,082 Btu/hr (9,400 W)
Avg Heat Input Rate per Foot of Bore	52.6 Btu/hr-ft (15.4 W/ft)
Circulator Flow Rate	10.1 gpm
Standard Deviation of Power	0.04%
Maximum Variation in Power	0.11%

LINE SOURCE DATA ANALYSIS

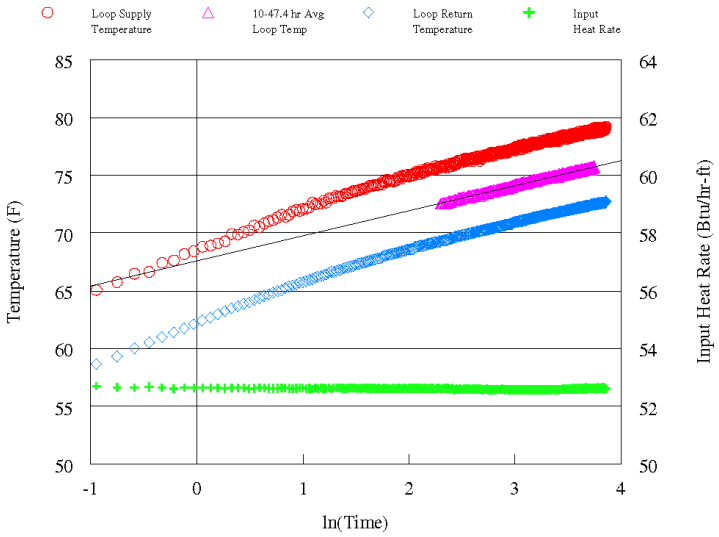

FIG. 2: TEMPERATURE & HEAT RATE VS NATURAL LOG OF TIME

The loop temperature and input heat rate data versus the natural log of elapsed time are shown above in Figure 2. The temperature versus time data was analyzed using the line source method (see page 3) in conformity with ASHRAE and IGSHPA guidelines. A linear curve fit was applied to the average of the supply and return loop temperature data between 10 and 42.5 hours. The slope of the curve fit was found to be 2.18. The resulting thermal conductivity was found to be **1.92 Btu/hr-ft-°F**.

THERMAL DIFFUSIVITY

The reported drilling log for this test borehole indicated that the formation consisted of fine sand and cobbles for overburden and gabbro and diorite bedrock. Average heat capacity values for gabbro and diorite were calculated from specific heat and density values listed by Kavanaugh and Rafferty[3]. A weighted average of heat capacity values based on the indicated formation was used to determine an average heat capacity of 36.1 Btu/ft^3-°F for the formation. A diffusivity value was then found using the calculated formation thermal conductivity and the estimated heat capacity. The thermal diffusivity for this formation was estimated to be **1.28 ft^2/day**.

[3] Stephen P. Kavanaugh and Kevin Rafferty, Geothermal Heating and Cooling: Design of Ground-Source Heat Pump Systems (Atlanta: ASHRAE, 2014), 75.

BORE THERMAL RESISTANCE

Resistance to heat transfer from a geothermal bore can be viewed as consisting of two components, bore resistance and ground resistance. This relationship is diagrammed in Figure 3, where t_f is the loop fluid temperature, t_b is the bore wall temperature and t_g is the ground temperature. The ground resistance is dependent upon the formation thermal conductivity and diffusivity. Factors that affect bore thermal resistance include the resistance of the pipe material, diameter of the heat exchanger, position of the heat exchanger in the bore, the bore diameter, casing length and type, and the thermal conductivity of the grout/backfill in the bore annulus. A detailed examination of bore resistance is discussed by Kavanaugh and Rafferty[4].

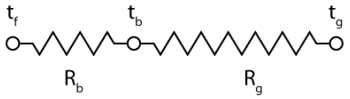

FIG. 3: RESISTANCE DIAGRAM FOR A GEOTHERMAL BORE

Bore thermal resistance calculations were made on the test data according to the formula below as outlined in the Gehlin Doctoral Thesis[5]. The calculated formation thermal conductivity and thermal diffusivity from the Line Source Analysis were used in the formula. The average undisturbed formation temperature of 53.8°F was used and the average bore thermal resistance from 10-42.5 hrs was found to be **0.236 hr-ft-°F/Btu** .

The calculated bore resistances apply only to the test conditions, and a bore in an operating loopfield could have a significantly different resistance due to changes in the loop fluid temperature, flow rate, and presence of antifreeze. Additional information on bore resistance may be found in the study by Oklahoma State University and Oklahoma Gas & Electric where various vertical bore heat exchanger configurations were tested[6].

$$R_b = \frac{H}{Q} * \left\{ T(t) - T_g - \frac{Q}{4\pi\lambda_g H} * \left[Ei\left(\frac{r_b^2}{4\alpha_g t}\right)\right]\right\}$$

Where:

	R_b	Borehole thermal resistance (hr-ft-°F/Btu)
	H	Active U-bend depth (ft)
	Q	Average heat injected (Btu/hr)
	$T(t)$	Temperature dependent on time t (°F)
	T_g	Undisturbed ground temperature
	λ_g	Formation thermal conductivity (Btu/hr-ft-°F)
	r_b	Average borehole radius (in)
	α_g	Formation thermal diffusivity (ft^2/hr)

[4]Stephen P. Kavanaugh and Kevin Rafferty, Geothermal Heating and Cooling: Design of Ground-Source Heat Pump Systems (Atlanta: ASHRAE, 2014), pages 58-67.
[5]Gehlin, 12-13.
[6] Beier, R. and Ewbank, G. (2012, August). *In-Situ Test Thermal Response Tests Interpretations, OG&E Ground Source Heat Exchange Study.* Retrieved from http://ghpok.org/